Cell Reports

Article

Histone deacetylase complex 1 facilitates hypocotyl elongation by attenuating acetylation and transcription via a PIF4-dependent process

Graphical abstract

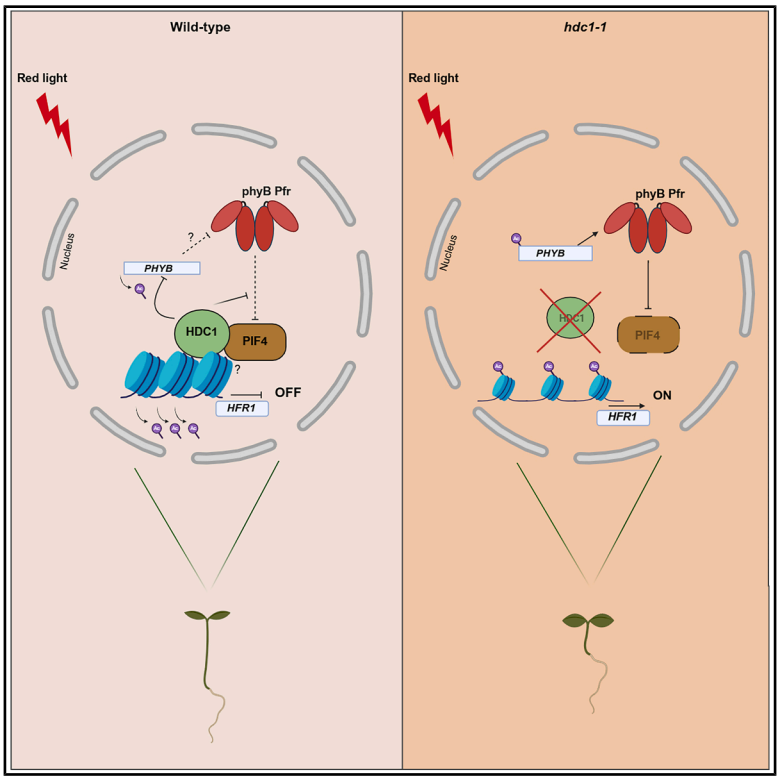

Authors

Weiwei Fang, Alessio Baldini, Gabriele Locci, ..., Riccardo Aiese Cigliano, Lucio Conti, Giorgio Perrella

Correspondence

giorgio.perrella@unimi.it

In brief

Light determines plant growth through the crosstalk between photoreceptors, downstream components and chromatin modifications. Fang et al. show that HDC1 attenuates transcriptional activation of phyB and other light-induced genes by deacetylating their promoter regions. Furthermore, HDC1 interacts with PIF4, and together they modulate gene expression to fine-tune photomorphogenesis in *Arabidopsis*.

Highlights

- HDC1 promotes hypocotyl elongation under red-light conditions
- HDC1 interacts and regulates PIF4 protein abundance
- HDC1 mediates (de)acetylation and expression state of phyB and other light-induced targets
- HDC1 and PIF4 co-regulate the expression of red-light-induced genes

Fang et al., 2025, Cell Reports *44*, 116027
August 26, 2025
https://doi.org/10.1016/j.celrep.2025.116027

CellPress

Cell Reports

CellPress
OPEN ACCESS

Article

Histone deacetylase complex 1 facilitates hypocotyl elongation by attenuating acetylation and transcription via a PIF4-dependent process

Weiwei Fang,[1,3] Alessio Baldini,[1,3] Gabriele Locci,[1] Filippo Battaglia,[1] Jaïr Dilmé Capó,[2] Santiago Radio,[2] Riccardo Aiese Cigliano,[2] Lucio Conti,[1] and Giorgio Perrella[1,4,*]

[1]Department of Biosciences, Università degli Studi di Milano, Via Celoria 26, 20133 Milan, Italy
[2]Sequentia Biotech SL, C/ del Dr. Trueta 179, 08005 Barcelona, Spain
[3]These authors contributed equally
[4]Lead contact
*Correspondence: giorgio.perrella@unimi.it
https://doi.org/10.1016/j.celrep.2025.116027

SUMMARY

Photomorphogenesis is a transitional response occurring when seedlings are exposed to light. Upon red-light exposure, this process depends on the nuclear translocation of phytochrome B (phyB) and its interaction with downstream components. Histone deacetylase complex 1 (HDC1) is a member of the histone deacetylation complex (HDAC) that regulates the sensitivity of *Arabidopsis* seedlings to environmental cues. Here, we show that HDC1 is a positive regulator of hypocotyl elongation when plants are exposed to red light. By employing protein interaction assays and mutant combinations, we demonstrate that HDC1 interacts with PIF4 and regulates its abundance. Chromatin immunoprecipitation sequencing (ChIP-seq) reveals that HDC1 modulates the expression of growth-promoting genes by deacetylating promoter regions and that HDC1 is required for PIF4 association over DNA targets. Altogether, our findings explore the connection between red-light signaling and chromatin states and assign another function to a member of the HDAC complex in plants.

INTRODUCTION

Light is one of the most important stimuli to fine-tune plant growth and developmental transitions. Light not only serves as an energy source for photosynthetic reactions but also triggers a series of signaling cascades occurring during adaptation to different environments. To sense light, plants have evolved separate photoreceptor families, each specialized in sensing a specific wavelength.[1,2]

Phytochromes (phyA–phyE) are red/far-red light receptors that are required for many aspects of plant development, including photomorphogenesis, also known as de-etiolation, which leads to shortening of hypocotyls and cotyledon opening. Phytochrome B is considered the main red-light receptor. Upon red-light stimulation, phyB activates a signaling cascade leading to the degradation of a group of helix-loop-helix transcription factors, known as PHYTOCHROME-INTERACTING FACTORS (PIFs), thereby triggering a transcriptional reprogramming that modulates photomorphogenesis.[3–5] When exposed to light, phytochromes interact with PIFs to trigger their phosphorylation, followed by ubiquitination and subsequent degradation, which, in turn, promote light-dependent gene expression.[6]

Histone acetylation is one of the post-translational modifications that causes heritable phenotypic changes by affecting chromatin accessibility without altering DNA sequence.[7,8] Histone (de)acetylation involves the addition or removal of acetyl groups to histones tails, which ultimately regulate transcriptional activation.[9,10] This reversible process is regulated by two classes of enzymes with antagonistic roles: histone acetyltransferases and deacetylases (HDAC).

Recent studies revealed histone acetylation as a key regulator of light-responsive gene networks. More specifically, H3K9 (de) acetylation is associated with light-induced gene repression and activation, respectively.[11–13] Additionally, histone deacetylase 15 (HDA15) can directly interact with PIF1 and PIF3 in the dark to suppress gene expression and facilitate photomorphogenesis.[14,15] PhyB has been shown to redundantly control chromatin remodeling to inhibit the transcriptional activation of growth-promoting genes by PIFs.[16,17] Besides photomorphogenesis, HDA15 has been shown to repress phyB-dependent seed germination in response to light through association with PIF1.[14] PIF3 also interacts with HDA15, and together they repress light-induced chlorophyll biosynthesis.[15] Finally, PIF7 upregulates shade-induced gene expression by allowing the deposition of H3K9ac and H3K14ac at different promoters.[18] Collectively, these studies indicate that light-induced responses are tightly regulated by chromatin states through histone modifications.

The genome-wide distribution of histone modifications was studied upon light-induced de-etiolation. Acetylation of H3K9 of the HY5 (ELONGATED HYPOCOTYL5) and HYH (HY5-HOMOLOG) loci was observed during dark-to-light transition,

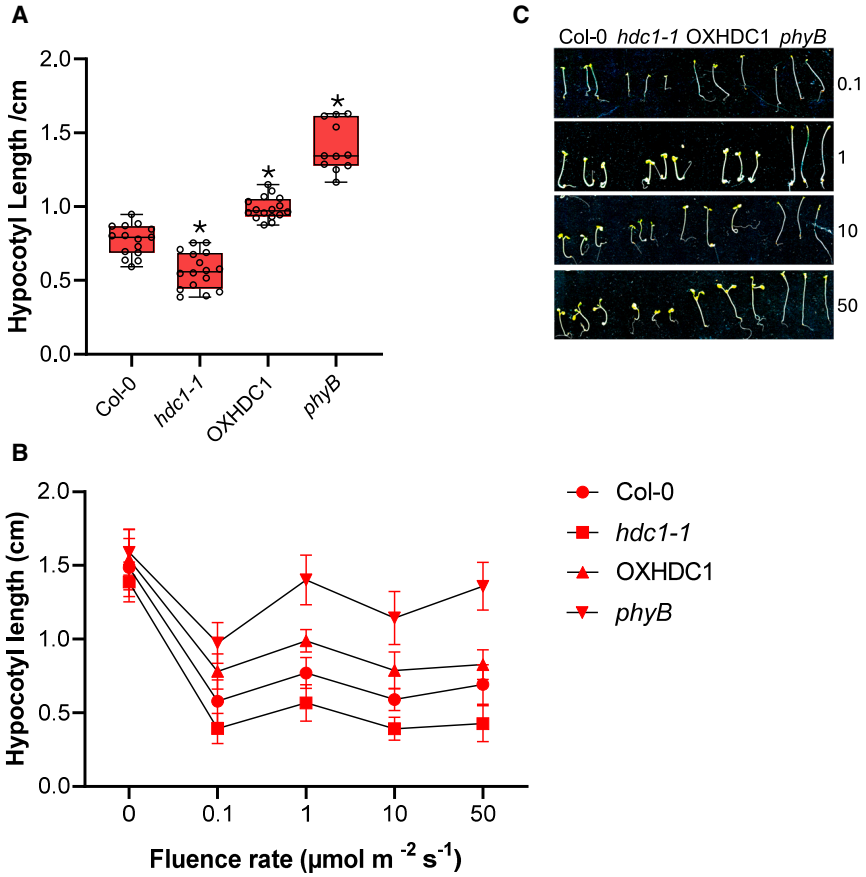

Figure 1. HDC1 promotes hypocotyl elongation of *Arabidopsis* seedlings under red-light conditions

(A) Hypocotyl measurements of Col-0, *hdc1-1*, and OX HDC1 under red light (1 μmol m^{-2} s^{-1}).

(B) Fluence response curve of Col-0, *hdc1-1*, and OX HDC1 under 0 (dark), 0.1, 1, 10, and 50 μmol m^{-2} s^{-1} of red light.

(C) Images of representative seedlings for the reported genotypes and light conditions. For each experiment, plants were grown for 5 days; *phyB* seedlings were used as positive controls for light conditions. Whisker plots display boxes with median, interquartile range (IQR), and maximum-minimum interval of each dataset ($n \geq 15$ seedlings). The IQR was calculated based on the following formula: quartile3 (Q3) – quartile1 (QI). Whiskers represent QI – 1.5 × IQR and Q3 + 1.5 × IQR.

Asterisks in (A) show significant differences for $p < 0.001$. One-way ANOVA showed significant differences between Col-0, *hdc1-1*, OXHDC1, and *phyB* at 0.1, 1, 10, and 50 μmol m^{-2} s^{-1} of red light ($p < 0.001$).

whereas acetylation of H3K27 was not monitored.[11] The deposition of histone marks such as H3K4me3, H3K9ac, H3K14ac and H3K27ac were correlated with phyA activation in the dark, while in light-grown seedlings, these marks were decreased.[19] The SWI-INDEPENDENT LIKE-HISTONE DEACETYLASE 19 complex has been reported to act as a negative regulator of photomorphogenesis via the HY5-dependent recruitment on light-signaling genes to repress their transcription.[20,21]

Histone deacetylase complex 1 (HDC1) is a component of the plant HDAC complex showing a partial homology to the yeast RPD3 large HDAC complex member RXT3. In *Arabidopsis*, HDC1 promotes histone deacetylation and acts as a transcriptional regulator. HDC1 mutations cause a range of phenotypes, including hypersensitivity to abiotic stress during germination, delayed flowering, and shortened petioles.[22,23] Conversely, overexpressing HDC1 desensitizes plants to ABA and salt and increases plant biomass under control and water-limited conditions. At the protein level, HDC1 interacts with a range of targets, including HDA6 and HDA19, the co-repressor SAP18, and the histone binding proteins ING2, MSI1, and SHL1. Additionally, HDC1 can also interact with the *Arabidopsis* H1 variants H1.1 and H1.2 and the stress-inducible H1.3 variant.[24,25]

In this study, we report that HDC1 is a positive regulator of hypocotyl elongation. We observed that the *hdc1-1* mutant displays significantly shorter hypocotyls specifically when exposed to red-light conditions. Expression analyses combined with chromatin immunoprecipitation (ChIP) revealed that HDC1 controls *PHYB* expression levels. Protein interaction and genetic analyses further indicate that HDC1 can directly interact with PIF4 and regulate its protein abundance. By combining ChIP with next-generation sequencing, we show that HDC1 can deacetylate promoter regions of growth-related genes in a H3K9K14 context. We also show that PIF4 requires HDC1 to bind DNA-regulatory regions to fine-tune gene expression. Thus, our findings reveal a mechanism for photomorphogenesis based on the crosstalk between histone deacetylation complex and light components and define a distinct function for HDC1 in plants.

RESULTS

HDC1 positively regulates red-light-mediated hypocotyl elongation

Previously, we have reported that HDC1 is required for seed germination in response to salt and ABA by deacetylating genes related to stress response.[22,24,25] Based on previous reports highlighting the role of HDACs in light signaling,[19] we hypothesized that HDC1 could have a broader role in mediating environmental signals, including photomorphogenesis. We therefore conducted hypocotyl growth assays using *hdc1* loss-of-function (*hdc1-1*) and *HDC1* overexpressing lines (*OX HDC1*) seedlings exposed to four monochromatic light conditions (red, blue, far-red, and dark) (Figures 1 and S1A–S1E). Unlike *hda19-2* mutants, where a response has been shown under different light qualities,[20] *hdc1-1* showed significantly shorter hypocotyls than the wild type exclusively under red-light conditions. Conversely,

OX HDC1 displayed longer hypocotyls under the same monochromatic light conditions (Figure 1). To further support our findings, we assessed hypocotyl elongation under different light fluences (0.1, 1, 10, and 50 μmol m^{-2} s^{-1}) for each light conditions (red, blue, and far-red). Again, *hdc1-1* and *OX HDC1* were consistently shorter and longer than the wild type only under red light exposure, respectively (Figures 1A–1C and S1). We therefore concluded that HDC1 can regulate photomorphogenesis primarily under red light, whereas its contribution under other light wavelengths is negligible (Figures S1B–S1E). Exposure to dark conditions also suggested that the hypocotyl elongation changes of *hdc1-1* (or OX HDC1) are not due to germination rate, supporting previous results displaying no defects under control conditions[22] (Figures 1 and S1).

To further confirm the function of HDC1 during hypocotyl elongation, we studied *HDC1* expression and distribution in seedlings of *Arabidopsis* using *pHDC1:GUS* lines (Figures S2A–S2D). Microscope observations of 1-week-old seedlings revealed *pHDC1*-driven GUS expression in cotyledons (Figures S2A and S2B), hypocotyls (Figures S2A–S2C), and roots (Figures S2A–S2D). These findings confirm previously obtained results corroborating that HDC1 is ubiquitously expressed in *Arabidopsis*.[22] The presence of GUS activity in hypocotyls further supports its putative role in hypocotyl growth. We also monitored *HDC1* gene expression and protein levels in Col-0 (wild-type [WT]) and GFP-tagged HDC1 seedlings, respectively, exposed to white light, red light, blue light, and darkness (Figure S2F). No major differences in *HDC1* transcript accumulation were observed under white, red, or blue light or even darkness conditions. GFP:HDC1 protein appeared to be unaffected by light qualities except that it was less abundant when plants were exposed to blue light, although no blue-light-specific defects were detected in *hdc1*/OX HDC1 with respect to hypocotyl elongation (Figures S1B–S1E).

Our results indicate that HDC1 might negatively regulate red-light-mediated photomorphogenesis. To test the impact of *HDC1* in red-light signal transduction, we generated double mutants of *hdc1-1* and mutants in the red-light receptor *phyB* (*phyB-9*) and its overexpression line (*OX phyB*) (Figure 2). The hypocotyl length of *hdc1-1 phyB* resembled that of *phyB*, suggesting that *phyB* is epistatic to *hdc1*. *OX phyB* plants showed an extremely short hypocotyl phenotype, confirming their enhanced photomorphogenic response to red light (Figure 2A). Double mutants of *OX phyB hdc1* exhibited no significant differences compared to *OX phyB* (one-way ANOVA, $p = 0.29$) (Figure 2A). Based on the enhanced photomorphogenic phenotype observed in *hdc1* plants, we then decided to assess whether HDC1 could affect endogenous *PHYB* levels. Total RNA was extracted from Col-0, *hdc1-1*, and *OX HDC1* seedlings that were dark adapted for 2 days and exposed to red light (10 μmol m^{-2} s^{-1}) for 5 h RT-qPCR analysis showed that *PHYB* transcripts were significantly increased in *hdc1* mutants compared to the other lines (Figure 2C, left). Similar results were obtained when we measured *PHYB* in OX phyB lines. Indeed, in the absence of HDC1, *PHYB* was increased even when under the control of a constitutive promoter, suggesting therefore a cumulative effect (Figure 2C, right). To evaluate whether higher *PHYB* expression is linked to its epigenetic state, we monitored H3K9K14 and H3K27 acetylation levels by ChIP assays coupled with qPCR. ChIP-qPCR results demonstrated an increase of acetylation in *hdc1* compared to Col-0 in three different promoter regions of the *PHYB* locus (Figures 2D–2F), indicating a positive correlation between expression and acetylation state. We next decided to investigate whether *hdc1* mutation might affect phyB nuclear bodies or protein abundance. First, we monitored nuclear bodies in 5-day-old seedlings exposed to red light. Confocal imaging showed no major differences in nuclear body formation between the two genotypes (Figure S3A). We then measured the number and size of nuclear bodies in *OX phyB:CFP* and *OX phyB:CFP hdc1* lines and observed no significant changes (Figures S3B and S3C). Subsequently, the detection of phyB protein levels in Col-0, *OX HDC1*, and *hdc1* showed similar levels of protein abundance and no significant changes (Figures S3D–S3F). The detection of phyB:CFP in both the WT and *hdc1* background revealed comparable results (Figures S3E–S3G). Taken together, our data indicate that HDC1 represses *PHYB* transcription by deacetylating its locus in response to red light, although protein levels were not affected. This highlights that phyB may be influenced by light-mediated changes in histone marks.

HDC1 interacts directly with PIF4 and stabilizes its protein abundance

Previous studies have demonstrated that phyB downstream components can recruit and interact with histone-modifying enzymes to coactivate genes and enhance chromatin modifications.[26] The PIF family is composed of basic-helix-loop-helix (bHLH) transcription factors that are implicated in hypocotyl elongation and seedling growth.[27] Among the PIFs, PIF4 and PIF5 are closely related to PIF3, as they present homology even outside of the bHLH domain.[28] PIF3 binds to both phyA and phyB, providing a role in both red and far-red photomorphogenesis.[29] PIF4 and PIF5 interact selectively with the biologically active phyB Pfr form, thereby acting specifically in the phyB signaling pathway.[30] In contrast, PIF1 is a key negative regulator of plant development, particularly in the dark.[14,31] Instead, PIF7 contributes primarily to hypocotyl elongation in response to shade avoidance and warm temperatures.[32–35] To address HDC1 involvement in the PIF4/5-dependent photomorphogenic responses, we first generated double mutants of *hdc1 pif4* and measured their hypocotyls under low-red-light conditions. As displayed in Figure 3A, compared to Col-0, *pif4* showed shorter hypocotyls. Interestingly, *hdc1 pif4* double mutants showed no significant difference in hypocotyl length when compared to *pif4*, suggesting that HDC1 may act through PIF4 (Figure 3A) (one-way ANOVA $p = 0.46$). Additionally, we obtained *pif4 pif5* double mutants and generated triple mutants with *hdc1*. Under red light, *pif4 pif5* seedlings showed extremely short hypocotyls, mimicking constitutive phyB-mediated signaling (Figure 3B). Interestingly, *hdc1* did not affect the *pif4 pif5* hypocotyl phenotype (one-way ANOVA $p = 0.97$), suggesting that HDC1, PIF4, and PIF5 may be involved in the same signaling pathway. Overexpressing HDC1 in the *pif4 pif5* background did not rescue the short hypocotyl phenotype, as the seedlings displayed the same hypocotyl length as *pif4 pif5* mutants, suggesting that HDC1

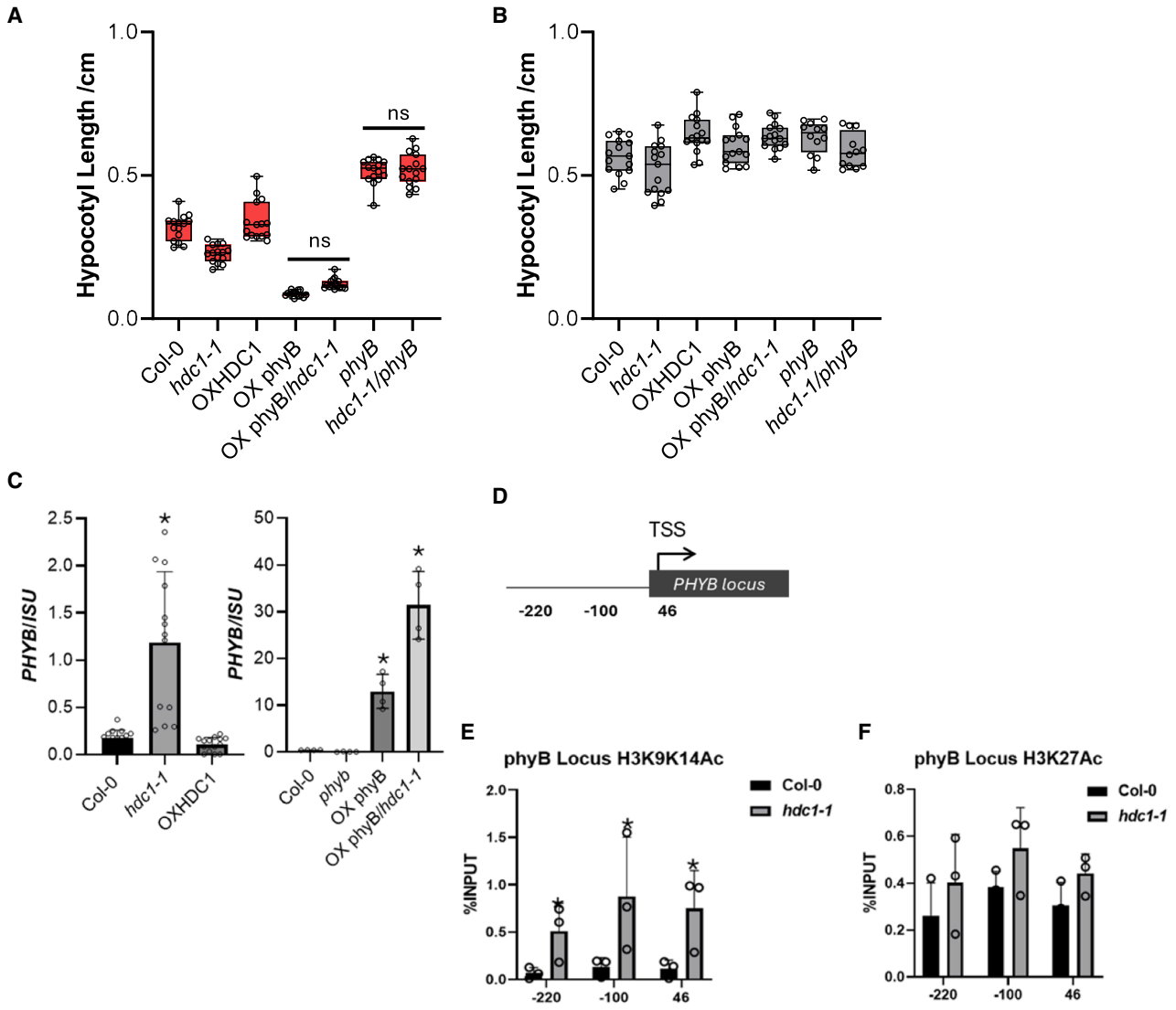

Figure 2. phyB is epistatic on HDC1, and the latter regulates its expression and acetylation levels

(A and B) Hypocotyl measurements of Col-0, *hdc1-1*, OX HDC1, and the reported double mutant and OX line combination under red (A) and dark (B) light conditions. Images of representative seedlings are shown in Figure S9. For (A), plants were grown for 5 days under red-light conditions (1 μmol m^{-2} s^{-1}). Whisker plots display boxes with median, IQR, and maximum-minimum interval of each dataset ($n \geq 15$ seedlings). The IQR was calculated based on the following formula: Q3 –QI. Whiskers represent QI – 1.5 × IQR and Q3 + 1.5 × IQR. Statistical analysis was performed between each combination with its own genetic background (one-way ANOVA).

(C) *PHYB* expression levels over *ISU* on 5-day-old Col-0, *hdc1-1*, and OX HDC1 (left) and Col-0, *phyB*, OX phyB, and OX phyB/*hdc1-1* (right) seedlings grown under red light (10 μmol m^{-2} s^{-1}).

(D) Schematic of the *phyB* locus and position of the amplicons used for ChIP-PCR.

(E and F) H3K9K14ac (E) and H3K27ac (F) levels on the depicted regions of the *phyB* locus as described in (D) in Col-0 and *hdc1-1*.

Asterisks indicate differences based on one-way ANOVA for p value < 0.05. Bars are mean ± SD of three biological replicates, reported above the bars.

requires PIF4 and PIF5 for full function (Figure 3B) (one-way ANOVA $p = 0.13$). Conversely, we also assessed the potential effect of HDC1 in controlling PIF4 function by comparing hypocotyl elongation under red light in PIF4-overexpressing *35S:PIF4:HA (PIF4-HA)* and *35S:PIF4:HA hdc1* (*PIF4-HA/hdc1-1*) lines. As reported previously, under these conditions *35S:PIF4:HA* plants showed longer hypocotyls compared with the WT.[36] This phenotype was significantly weakened in the *hdc1* mutant background (Figure 3C), whereas no effect was recorded in the dark for all of the different mutant combinations evaluated (Figures 3D–3F).

To investigate whether HDC1 could directly affect PIF functions, we conducted bimolecular fluorescence complementation (BiFC) assays in *Nicotiana Benthamiana* epidermal leaves. We used the 2-in-1 system,[37] where the same vector contains HDC1 fused to the N terminus of yellow fluorescent protein (YFP), with the C terminus either fused to PIF4 or PIF5. RFP signal detection allowed

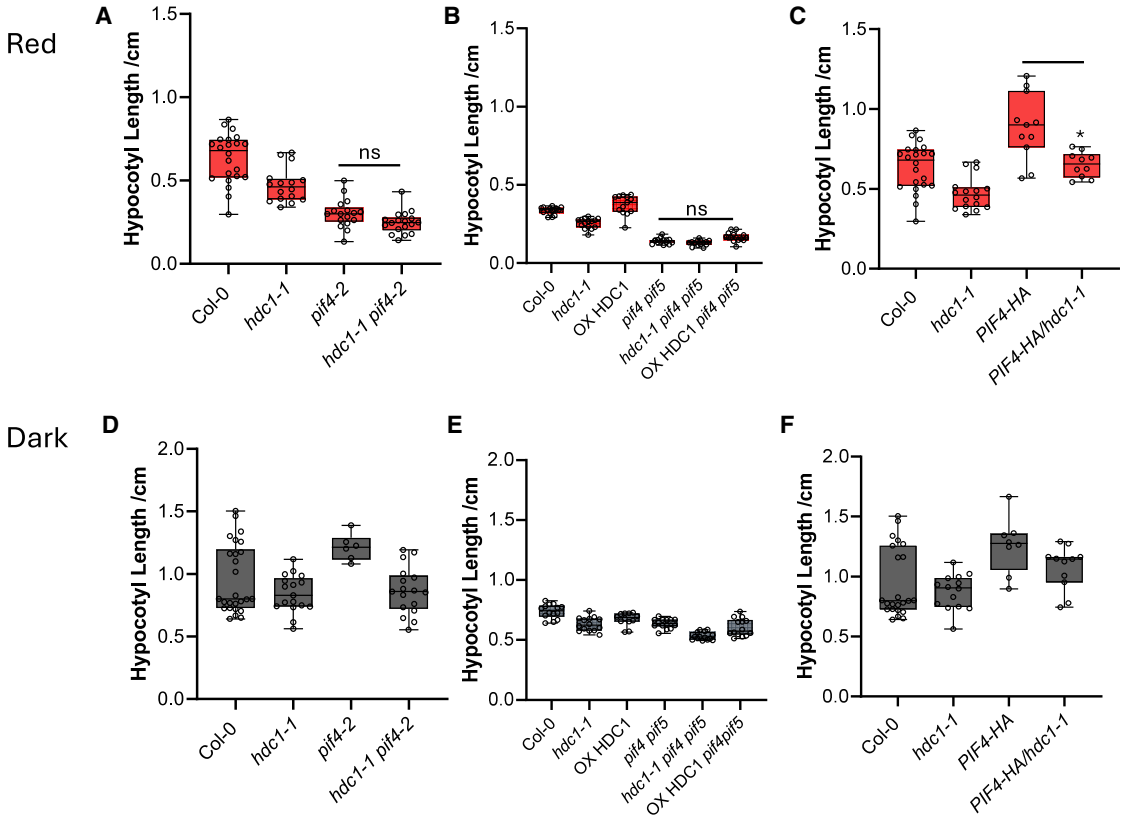

Figure 3. HDC1 requires PIFs for function during hypocotyl elongation

Hypocotyl measurements of Col-0, *hdc1-1*, *pif4-2*, *pif4/pif5*, *PIF4:HA*, and the reported double-mutant and OX line combination under red (A–C) and dark (D–F) light conditions. For (A)–(C), plants were grown for 5 days under red-light conditions (1 μmol m^{-2} s^{-1}). Whisker plots display boxes with median, IQR, and maximum-minimum interval of each dataset ($n \geq 15$ seedlings). The IQR was calculated based on the following formula: Q3 – quartile1 QI. Whiskers represent QI – 1.5 × IQR and Q3 + 1.5 × IQR. Statistical analysis was performed between each combination with its own genetic background (one-way ANOVA). Asterisk indicates differences at $p < 0.05$.

for an internal control to identify transformed cells (Figure 4A), whereas BiFC of HDC1 and H1 was used as a positive interaction control.[24] As reported in Figure 4B, a strong YFP signal was detected in the nucleus when HDC1 was co-infiltrated together with PIF4, suggesting interaction. Interestingly, no YFP signal was detected when HDC1 was co-expressed with PIF5, suggesting that the HDC1-PIF4 interaction is specific. We also assessed the interaction between PIF4 or PIF5 and the HDC1 RXT3 domain (RXT3L) which is partially required for HDC1 function (Figure 4B).[24] Similar to HDC1 full length, RXT3L reconstituted a YFP signal with PIF4 but not PIF5, thus confirming HDC1-PIF4 binding and suggesting that the interaction might occur via the RXT3 domain. Additionally, colocalization studies confirmed that both HDC1 and PIF4 reside primarily in the nucleus when co-expressed (Figure S6A). We further examined the interaction between HDC1 and PIF4 by co-immunoprecipitation (coIP) assay both in *Arabidopsis* (Figures 4C and 4D) and *N. benthamiana* (Figure S6B). In *Arabidopsis*, 5-day-old Col-0, GFP-HDC1, and *pif4 pif5* seedlings were dark adapted and exposed to red light for 5 h, (10 μmol m^{-2} s^{-1}). Proteins were immunoprecipitated using an anti-GFP and an anti-PIF4 antibody for immunoblot analysis. GFP-HDC1 could co-immunoprecipitate PIF4 in the WT but not in the *pif4 pif5* background. Similarly, in *N. benthamiana* leaves exposed to the same light conditions, PIF4 fused to RFP was found in the GFP-HDC1 immunoprecipitated fractions (Figure S6B).

Under red light, phyB can directly interact with and trigger PIF4 degradation.[16,38] Based on the interaction data and the OX HDC1 long hypocotyl phenotype (Figure 1), we postulated that the HDC1-PIF4 interaction might prevent PIF4 degradation, while in the absence of HDC1, PIF4 levels could be more destabilized. To verify this hypothesis, western blotting was performed to assess PIF4 levels in Col-0, OX HDC1, and *hdc1-1* seedlings grown for 5 days, dark adapted, and then exposed to red light for 5 h (10 μmol m^{-2} s^{-1}) or constantly kept in the dark. We detected a significant increase in PIF4 levels in OX HDC1 when compared to Col-0, while a reduction was observed in *hdc1*, further corroborating our hypothesis that HDC1 may regulate PIF4 protein levels (one-way ANOVA, $p \leq 0.05$) (Figures 4E and 4F). Under dark conditions, we did not observe any reduction in PIF4 levels in *hdc1-1*, suggesting that it is caused mainly by red light exposure (Figure S8A). Taken together, we demonstrated that HDC1 directly interacts with PIF4 and may be required to define its protein abundance during photomorphogenesis.

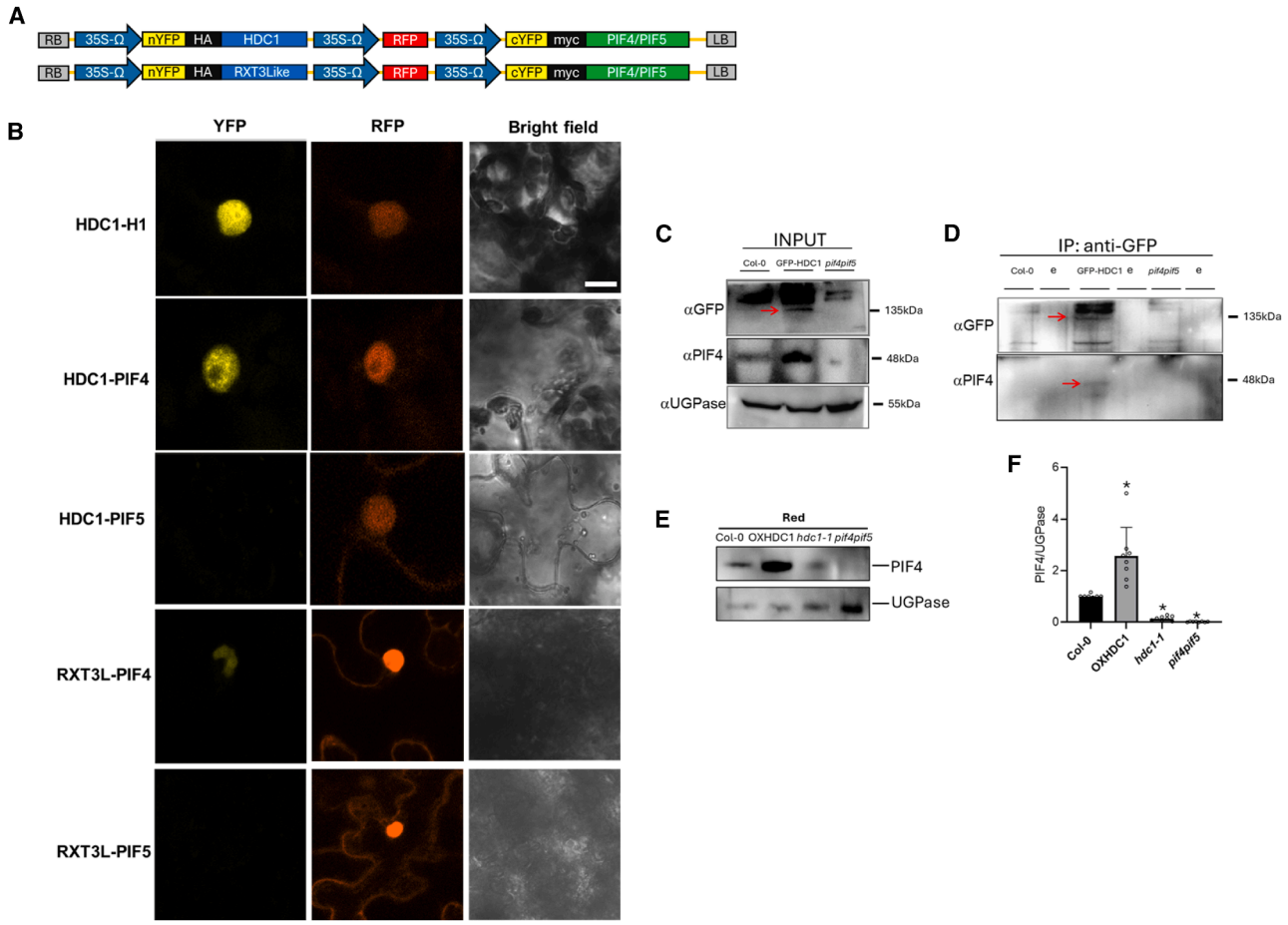

Figure 4. HDC1 directly interacts with PIF4 and determines its protein abundance

(A) Schematic of the 2-in-1 vector for BiFC containing N- and C-terminal halves of YFP signals fused to each protein and full-length RFP.

(B) Representative YFP signals in nuclei of *N. benthamiana* epidermis cells transformed with the indicated vectors and protein pairs. Scale bar: 10 μm.

(C and D) *In vivo* coIP of GFP HDC1 and PIF4. Proteins were extracted from 5-day-old *Arabidopsis* plants overexpressing GFP HDC1 exposed to red light (10 μmol m^{-2} s^{-1}). HDC1 and PIF4 were detected by using anti-GFP and anti-PIF4, respectively. GFP HDC1 was immunoprecipitated by using anti-GFP beads. The anti-UGPase signal was detected as a loading control. Col-0 and *pif4/pif5* seedlings were used as negative control. Red arrows indicate GFP and PIF4 signals, respectively. "e" are empty wells.

(E) Western blot analysis of PIF4 protein levels in 5-day-old Col-0, OX HDC1, *hdc1-1*, and *pif4/pif5* seedlings exposed to red light (10 μmol m^{-2} s^{-1}). PIF4 levels were detected by anti-PIF4 antibody. The UGPase signal was detected as a loading control.

(F) Quantification of PIF4 signal over UGPase under red light for the genotypes and conditions reported in (E). Data are mean ± SD of eight biological replicates, reported above the bars. Asterisks show significant differences for $p < 0.05$ to Col-0 (one-way ANOVA).

HDC1 determines the deacetylation and transcriptional state of light-responsive genes

To pinpoint targets of HDC1-mediated deacetylation, we isolated nuclei from 5-day-old Col-0 and *hdc1-1* seedlings exposed to red light and performed ChIP with antibodies against acetylated lysine 9, 14, and 27 in histone 3 (anti-H3K9K14Ac and anti-H3K27Ac) respectively, followed by sequencing. For each genotype, two biological replicates were analyzed for each antibody used (Figures S4A–S4E). Using a false discovery rate of 0.05, we identified 3,892 differentially expressed peaks between Col-0 and *hdc1* for H3K9K14Ac and 100 for H3K27Ac, respectively (Data S2 and S3; Figure S4A). In accordance with published histone acetylation distributions, the majority of the differentially enriched peaks were located in promoter regions, within 1–2 kb of the TSS (Figures S4C and S4D). Gene Ontology analysis of the differentially acetylated regions between *hdc1-1* and Col-0 showed no enrichment for H3K27Ac, as only three categories for few hypoacetylated genes were identified (Figure S5A). Conversely, the analysis of up-H3K9K14Ac using the same criteria revealed a significant enrichment in *hdc1-1* for targets related to light intensity, photosynthesis, and response to red or far-red light. Promoter regions that appeared hypoacetylated in *hdc1-1* were instead associated with genes involved in salicylic acid, hypoxia, and low oxygen signaling (Figure S5B).

Four genes were selected for more detailed analysis based on the preferential expression under red-light and their role in photomorphogenesis. *LONG HYPOCOTYL IN FAR RED* (*HFR1*;

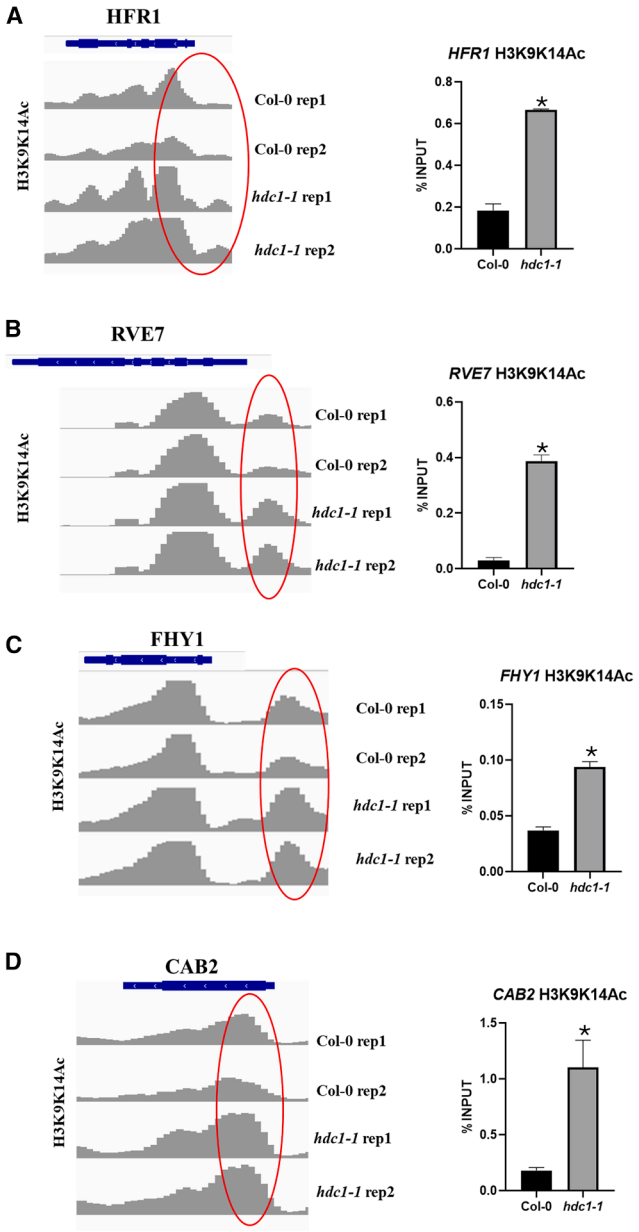

Figure 5. HDC1 attenuates H3K9K14 acetylation of HFR1, RVE7, FHY1 and CAB2 under red light conditions

H3K9K14ac coverage on four genes in Col-0 and *hdc1-1* seedlings grown under red-light conditions (10 μmol m^{-2} s^{-1}).

Shown are (A) *HFR1* (AT1G02340), (B) *RVE7* (AT1G18330), (C) *FHY1* (AT2G37678), and (D) *CAB2* (AT1G29920). The ChIP-seq profiles show normalized read numbers over 200-bp windows for two experimental replicates per genotype. Genes with 3′/5′ UTRs are represented as boxes, and white arrowheads indicate the direction of transcription. Red circles indicate the position of primers used for ChIP-qPCR and differential enrichment in common peaks identified using DiffBind. The graphs on the right of each plot amount of anti-H3K9K14ac ChIP DNA determined by qPCR in percent of input. Bars are means of 4 technical replicates ± SD on a third experimental replicate. For ChIP experiments, ~3,000 seedlings per genotype under red light were processed for a total of three independently grown batches. Two biological replicates were subjected to sequencing, while a third one was analyzed by ChIP-qPCR. Asterisks show significant differences for $p < 0.05$ to Col-0 (t test). Plant material was obtained from 5-day-old Col-0 and *hdc1-1* seedlings.

AT1G02340) is a transcription factor with a bHLH domain acting downstream of both phytochromes and cryptochromes.[39] *REVEILLE 7* (*RVE7*; AT1G18330) is a transcription factor involved in phytochrome-dependent cotyledon expansion.[40,41] *FAR-RED ELONGATED HYPOCOTYL 1* (*FHY1*; AT2G37678) also inhibits hypocotyl elongation by directly binding to photoreceptors.[42–44] *CHLOROPHYLL A/B-BINDING PROTEIN* (*CAB2*; AT1G29920) is involved in photosynthesis and light perception, and its expression is regulated by environmental changes[45] (Figures 5A–5D). An independent ChIP-qPCR on the promoter regions of these genes confirmed the differential accumulation of histone marks (Figures 5A–5D) and determined the specificity of HDC1 for H3K9K14 acetylation residues.

To compare acetylation profiles with the expression of the selected genes, we also measured transcript levels using RT-qPCR. The results revealed a strong accumulation of these genes under red-light conditions in *hdc1* mutants compared with the WT (one-way ANOVA, $p \leq 0.05$), whereas OX HDC1 lines did not show significant deregulation compared with the WT (Figures 6A–6D). It is worth noting that we measured expression levels of other growth-related genes, including *ATHB2*, *HY5*, and *HYH*[46–48] (Figures 6E–6G). Interestingly, although they are not present in our ChIP-seq datasets, these genes also showed an opposite pattern between *hdc1-1* and OX HDC1, although not present in our ChIP-seq datasets, suggesting that HDC1 could also indirectly regulate their expression (Figures 6E–6G). In summary, red light increases histone acetylation and transcript levels of responsive genes, and both responses are dampened by HDC1.

HDC1 and PIF4 coordinate the expression of photomorphogenesis genes

Given the interaction between HDC1 and PIF4 and the HDC1-mediated deacetylation of red-light-induced genes, we were prompted to investigate whether HDC1 and PIF4 could converge to regulate common targets. By overlapping published PIF4 ChIP-seq datasets[49] and differentially enriched ChIP peaks in *hdc1*, we could correlate PIF4 binding sites and the HDC1-mediated differential acetylation peaks for the marks reported above (H3K9K14ac and H3K27ac) (Data S4–S6). Altogether, we found 12 genes that were shared among the three datasets. Notably, a significant number of targets (931) was specifically enriched between PIF4 and differential H3K9K14Ac (WT vs. *hdc1-1*) (Data S4–S6). Among them, we found *HFR1*, *RVE7*, and *FHY1*, which we confirmed as direct targets of HDC1-mediated deacetylation. The PIF4 ChIP-seq dataset further revealed a general association with promoter and TSS regions of these targets with an overlap with HDC1 H3K9K14 acetylation peaks (Figure S7).[49] To test the requirement of HDC1 in promoting PIF4 binding to these promoter regions, we performed ChIP-qPCR on *35S:PIF4:HA* and *35S:PIF4:HA hdc1* lines. Using an anti-hemagglutinin (HA) antibody, we could show comparable levels of PIF4:HA accumulation in

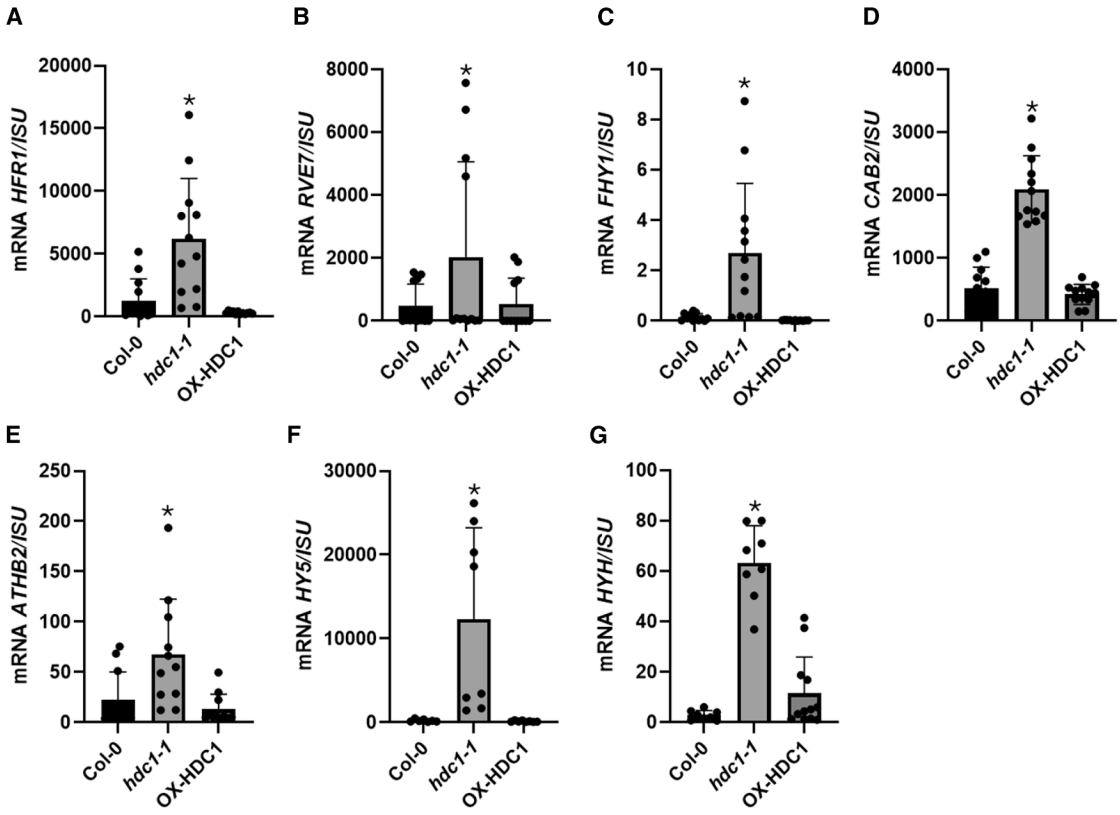

Figure 6. HDC1 moderates transcription levels of growth-promoting genes under red-light conditions

Shown are mRNA levels of *HFR1* (A), *RVE7* (B), *FHY1* (C), *CAB2* (D), *ATHB2* (*AT4G16780*) (E), *HY5* (*AT5G11260*) (F), and *HYH* (*AT3G17609*) (G) in 5-day-old seedlings of Col-0, *hdc1-1*, and OX HDC1 grown on control medium under red-light conditions, determined by qPCR and normalized to the housekeeping gene *ISU*. Bars are means of 3 independent biological replicates (reported above the bars as technical replicates) ± SD. Asterisks indicate differences at $p < 0.05$ (one-way ANOVA). For each biological replicate, ~150 seedlings per genotype were processed.

these lines, ruling out a potential effect of HDC1 in the control of transgene accumulation (Figure S8B). The ChIP-qPCR assay performed on three biological replicates confirmed PIF4 association with different upstream regions of *HFR1*, *REV7*, and *FHY1*, respectively (Figures 7B–7D). However, in *hdc1* mutants, PIF4 association with DNA was significantly diminished, suggesting that PIF4 recruitment to the regulatory regions of these targets is dependent on the presence of HDC1 (Figures 7B–7D). We also assessed whether HDC1 could directly bind the regulatory regions of these reported targets. Thus, we immunoprecipitated chromatin from GFP-HDC1 seedlings using an anti-GFP antibody and performed qPCR on *HFR1*, *FHY1*, and *RVE7* promoters. Interestingly, no enrichment was observed when compared to the negative control Col-0 (Figure 7B). Altogether, the data highlight the importance of the HDC1-PIF4 interaction in modulating gene expression, primarily in response to red light in *Arabidopsis*.

DISCUSSION

HDC1 modulates hypocotyl elongation by contributing to phyB-mediated signaling

Changes in chromatin state determine transcription factor (TF) accessibility and gene expression regulation in response to environmental changes.[50] It is still unclear how, following photoreceptor translocation to the nucleus, their signaling is regulated depending on the chromatin environment to fine-tune plant growth.

Transcriptional regulation is the basis of photomorphogenesis, and it is controlled by a small number of TFs, including the master regulator HY5 and the family of PIFs. Each TF, in turn, controls hundreds of genes involved in different light-regulated pathways, all converging in light-controlled subnuclear hubs.[51–53] Furthermore, a vast array of epigenome modifiers, including ATP-dependent chromatin remodelers, histone chaperones, or histone-modifying enzymes, act in cooperation or independent of transcriptional regulators to ultimately shape the (epi)genome landscape under fluctuating light conditions, thereby influencing transcription and chromatin architecture.[54,55]

In this study, we showed that HDC1, a scaffold protein that is an essential component of the HDAC complex, is required to promote hypocotyl elongation and to modulate the expression of growth-promoting genes in a red-light-specific manner. Previous studies have shown that HDC1 co-elutes with HDA19, an important repressor of photomorphogenesis.[20,56] However, while HDA19 photomorphogenic responses are not dependent on light quality, our data suggest that HDC1 is required primarily

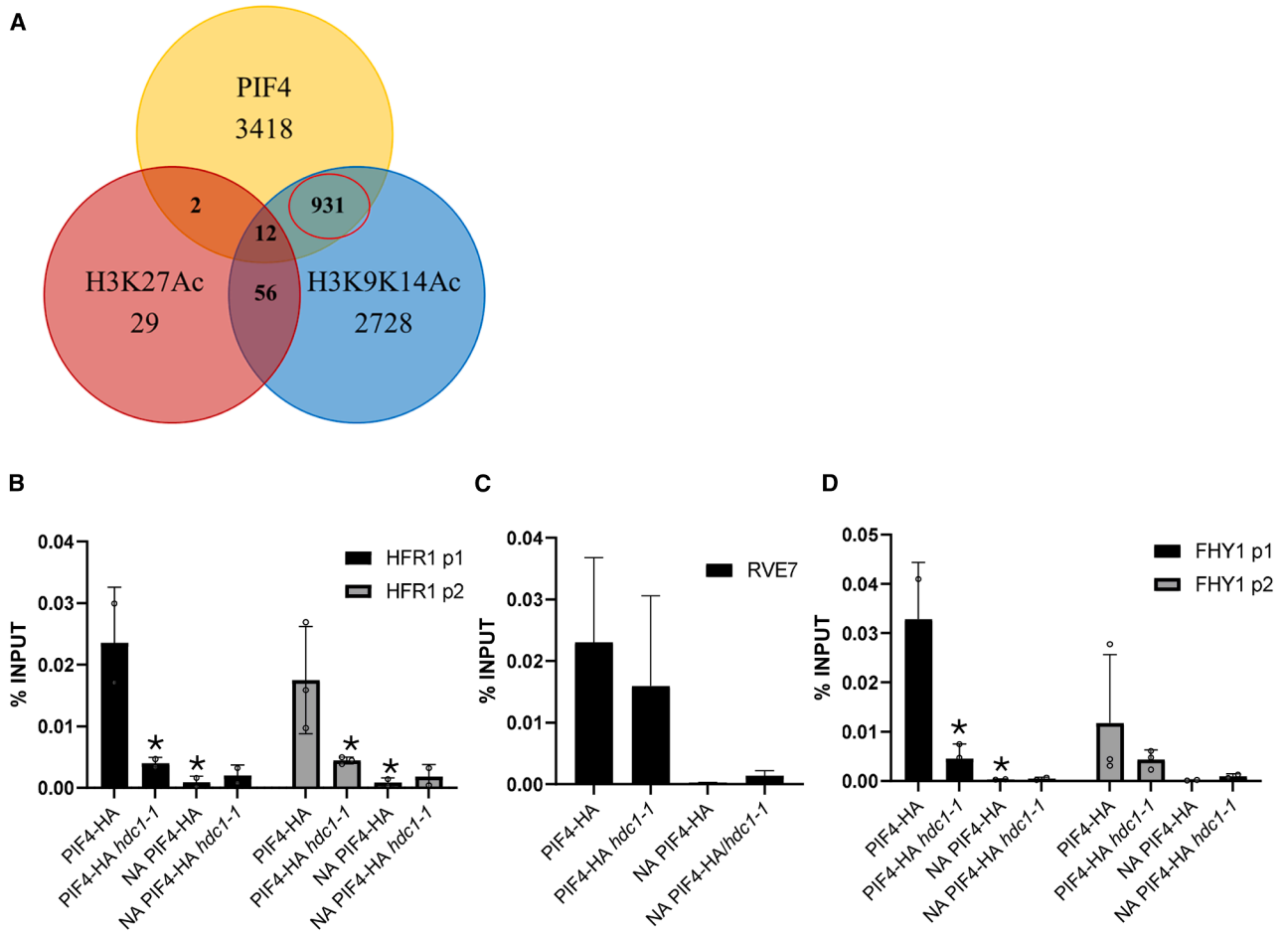

Figure 7. PIF4 and HDC1 modulate photomorphogenesis by regulating a subset of growth-related targets

A Venn diagram (A) depicts the common and individual targets bound by PIF4 and the differentially acetylated targets between Col-0 and *hdc1-1* for H3K27Ac and K9K14Ac by HDC1 (B–D). ChIP-qPCR depicts PIF4 binding on promoter regions of *HFR1* (B), *RVE7* (C), and *FHY1* (D) in PIF4:HA and PIF4:HA/*hdc1-1* seedlings exposed to red light. Non-antibody (NA) samples in PIF4:HA and PIF4:HA/*hdc1-1* were used as a negative control. Bars are mean ± SD of three biological replicates, reported above the bars. Amplified regions are shown in Figure S7. Data in (B)–(D) are mean ± SD of three biological replicates. Statistical analysis was performed between each combination with its own genetic background (two-way ANOVA). Asterisks indicate differences at $p < 0.05$.

for red-light signaling, indicating a more specific action compared to HDAC (Figure 1). HDC1 has been reported previously to interact with both HDA6 and HDA19[22]; however, we cannot exclude that HDAC complex composition is influenced by light quality.

Our data showed that phyB is epistatic to HDC1 and that *PHYB* expression and acetylation levels were negatively regulated by HDC1, indicating a different mode of action to modulate the photoreceptor signaling pathway (Figure 2). Histone acetylation, which is usually associated with an increase in gene expression, has been shown previously to be involved in the expression of light-responsive genes.[15,57,58] The *PHYA* locus shows reversible histone acetylation during dark-to-light transition, with a tug-of war between acetylated and methylated regions, which, in turn, induces/represses *PHYA* expression.[19] Additionally, our data indicate that HDC1 does not affect phyB protein abundance, neither nuclear body size nor number, suggesting that HDC1 functions primarily via transcriptional regulation. However, we cannot rule out that phyB turnover could occur on a different timescale. It would be interesting indeed to assess phyB protein abundance in a time-of-the-day manner.

PIF4 is the main integrator of the red-light signaling pathway, and it is negatively regulated by phyB.[38] Our combined genetic and protein studies demonstrate that HDC1 and PIF4 interact to fine-tune hypocotyl length. Interestingly PIF4 maintains interaction with the RXT3 HDC1 domain that shows homology to the yeast protein that co-elutes with the RPD3 complex.[59] This indicates that the RXT3 domain may preserve some of the HDC1 roles during light perception and suggests similar functions in other organisms. Further investigations are required to address this question and define which PIF4 domain(s) are important for interaction and whether other PIFs might be involved. Our experiments indicate that PIF4 endogenous protein levels were decreased in *hdc1-1* compared to the WT. This might suggest that HDC1 may protect PIF4 from the phyB-dependent degradation, as observed in OX HDC1. Analyses of *hdc1-1/pif4/pif5* triple

and *hdc1/pif4-2* double mutants allowed us to position PIF4 downstream of HDC1 (Figure 3). Decreased levels of PIF4 lead to the inactivation of growth-promoting genes and, thus, to the inhibition of hypocotyl growth.[60]

HDC1 deacetylates light-inducible genes and is required for PIF4 association with the DNA

Hypocotyl elongation can be modulated by HDC1 through deacetylation, hence repressing genes that favor expansion. While K9K14 is a canonical HDAC target, K27 appears to be modified during light exposure of light components. Our results showed changes in *hdc1* acetylation primarily for K9K14, with over 3000 targets being differentially modified, while only 100 targets were identified for K27. We could therefore conclude that HDC1 works mainly on the former, thereby suggesting changes in the histone code based on acetylation position. A closer look at the targets being identified allowed us to highlight a clear distinction between the hyperacetylated (UP in *hdc1-1* vs. Col-0) and the hypoacetylated regions (DOWN in hdc1-1 vs. Col-0). Indeed, Gene Ontology analysis indicated targets involved in light intensity, photosynthesis, and red light in the former, while the latter comprises annotations such as response to salicylic acid and hypoxia (Figure S4). The combined results reflect the role of HDC1 during the deacetylation process and further consolidate its function to attenuate gene expression under red-light conditions. This hypothesis was further confirmed by the genes identified in the process. In fact, targets like *HFR1*, *RVE7*, *FHY1*, and *CAB2* are well-established regulators of hypocotyl elongation that depend on light quality (Figures 5 and 6). Interestingly, *hfr1* mutants display long hypocotyls under low-light conditions.[61]

The crosstalk between light components and chromatin mainly occurs downstream on primary targets. Our observation implies that PIF4 and HDC1 are both required on the same regulatory regions or that HDC1 might allow PIF4 DNA binding (Figures 7 and S7A). To test this hypothesis, we introgressed *hdc1* in the *35S:PIF4:HA* background and assessed its effect both at the phenotypic and molecular levels (Figure 3C). Interestingly, in case of *35S:PIF4:HA*, *hdc1* mutation does not seem to affect protein levels, thereby ruling out any effect due to a difference in the expression of the tagged PIF4. Our results suggest that PIF4:HA can only partially counteract HDC1 deficiency; thus, PIF4 requires HDC1 for full function. Similarly, PIF4 binding over shared regulatory regions of the common targets is significantly diminished in the absence of HDC1 (Figure 7). It is therefore plausible that the HDC1-dependent deacetylation is a prerequisite for subsequent PIF4 binding, considering that HDC1 might not bind DNA elements directly (Figure S7B). Thus, HDC1-mediated deacetylation might occur before the induction of those genes, in an opposite manner to what concerns stress responses.[25] Whether this is a general effect or it is restricted on a few targets remains to be explored.

In summary, we propose that HDC1 presents a dual function to fine-tune hypocotyl elongation. At the transcriptional and chromatin levels, it modulates the expression of light components, including the photoreceptor phyB and light-induced genes like *HFR1* and other targets. Additionally, HDC1 interacts with and recruits PIF4 on chromatin regions. In the absence of HDC1, the hyperacetylation status allows an increase in gene expression and phyB-dependent PIF4 degradation (Figure S10). This mechanism reinforces the concept of HDC1 as a rate-limiting component of the HDAC complex and encourages the use of HDC1 to generate innovative epi-alleles through gene editing to optimize plant growth.

Limitations of the study

Our study reveals that HDC1 promotes hypocotyl elongation under red light by attenuating phyB expression and that it is important to modulate PIF4 and its recruitment to gene promoters. However, at this stage, we were not able to fully demonstrate how HDC1-mediated acetylation regulates phyB. Our results showed no changes in phyB abundance or nuclear body formation (Figure S3), but it does remain unclear whether or how it affects the photoreceptor post-translationally. In this work, we focused primarily on the mutual interaction between HDC1 and PIF4. Thus, future experiments will aim to investigate the mode of action between HDC1 and other PIFs, including PIF3, which is also required for hypocotyl elongation under red-light conditions; this comprises assessing the putative HDC1-PIF3 interaction and association with DNA as well as analyzing *hdc1/pif3* double-mutant lines.

RESOURCE AVAILABILITY

Lead contact

Requests for further information, resources, and reagents should be directed to and will be fulfilled by the lead contact, Giorgio Perrella (giorgio.perrella@unimi.it).

Materials availability

Plant materials and plasmids generated in this study will be available upon request. This study did not generate new unique reagents.

Data and code availability

- The raw and processed ChIP-seq data generated in this study have been deposited in BioProject: PRJNA1191197 (https://www.ncbi.nlm.nih.gov/bioproject/PRJNA1191197).
- No original code was generated in this study.
- Any additional information required to reanalyze the data reported in this paper is available from the lead contact upon request.

ACKNOWLEDGMENTS

We thank Dr. Eirini Kaiserli and Martijn Van Zanten for providing *phyB-9*, *pif4 pif5*, *35S:phyB-CFP*, *pif4-2*, and *35S:PIF4-HA* seeds. We thank the NOLIMITS core facility at the University of Milan for the microscopy imaging support. This work was funded by University of Milan research grants PSR2022 and My First Seed PSRL324. L.C. is supported by the Italian Ministerial of Research PRIN 2022 "Light and drought signal integration driving development transitions and adaptations in plants – LIDS," (Ref: 2022T2737Y). W.F. was funded by a post-doctoral fellowship of the University of Milan. A.B. is funded by a PhD fellowship from the University of Milan. F.B. is supported by the My First Seed PSRL324 scholarship. The authors acknowledge support from the University of Milan through the APC initiative. The graphical abstract was created in BioRender (https://BioRender.com/c78s599).

AUTHOR CONTRIBUTIONS

W.F., A.B., and G.P. conceived and designed the research. W.F., A.B., G.L., F. B., and G.P. performed experiments. J.D.C., S.R., R.A.C., and G.P. analyzed the ChIP-seq data and performed bioinformatic analyses. W.F., A.B., L.C.

and G.P. wrote the manuscript. All the authors read, revised, and approved the manuscript.

DECLARATION OF INTERESTS

J.D. and S.R. are employees of Sequentia Biotech SL. R.A.C. is scientific director and co-founder of Sequentia Biotech SL.

STAR★METHODS

Detailed methods are provided in the online version of this paper and include the following:

- KEY RESOURCES TABLE
- EXPERIMENTAL MODEL AND STUDY PARTICIPANT DETAILS
- METHOD DETAILS
  - Plant materials and growth conditions
  - Hypocotyl measurements
  - qRT-PCR analysis
  - Western blotting
  - BiFC
  - Co-IP
  - Chromatin immunoprecipitation (ChIP) and ChIP PCR
  - ChIP sequencing and data processing
  - Confocal imaging and analysis
- QUANTIFICATION AND STATISTICAL ANALYSIS

SUPPLEMENTAL INFORMATION

Supplemental information can be found online at https://doi.org/10.1016/j.celrep.2025.116027.

Received: December 20, 2024
Revised: May 6, 2025
Accepted: June 27, 2025

REFERENCES

1. Galvão, V.C., and Fankhauser, C. (2015). Sensing the light environment in plants: photoreceptors and early signaling steps. Curr. Opin. Neurobiol. *34*, 46–53. https://doi.org/10.1016/j.conb.2015.01.013.
2. De Wit, M., Galvão, V.C., and Fankhauser, C. (2016). Light-Mediated Hormonal Regulation of Plant Growth and Development. Annu. Rev. Plant Biol. *67*, 513–537. https://doi.org/10.1146/annurev-arplant-043015-112252.
3. Pham, V.N., Kathare, P.K., and Huq, E. (2018). Phytochromes and Phytochrome Interacting Factors. Plant Physiol. *176*, 1025–1038. https://doi.org/10.1104/pp.17.01384.
4. Wang, Z., Wang, W., Zhao, D., Song, Y., Lin, X., Shen, M., Chi, C., Xu, B., Zhao, J., Deng, X.W., and Wang, J. (2024). Light-induced remodeling of phytochrome B enables signal transduction by phytochrome-interacting factor. Cell *187*, 6235–6250.e19. https://doi.org/10.1016/j.cell.2024.09.005.
5. Cai, X., and Huq, E. (2025). Shining light on plant growth: recent insights into phytochrome-interacting factors. J. Exp. Bot. *76*, 646–663. https://doi.org/10.1093/jxb/erae276.
6. Chen, M., and Chory, J. (2011). Phytochrome signaling mechanisms and the control of plant development. Trends Cell Biol. *21*, 664–671. https://doi.org/10.1016/j.tcb.2011.07.002.
7. Pfluger, J., and Wagner, D. (2007). Histone modifications and dynamic regulation of genome accessibility in plants. Curr. Opin. Plant Biol. *10*, 645–652. https://doi.org/10.1016/j.pbi.2007.07.013.
8. Fang, W., Fasano, C., and Perrella, G. (2023). Unlocking the Secret to Higher Crop Yield: The Potential for Histone Modifications. Plants *12*, 1712. https://doi.org/10.3390/plants12081712.
9. Ouyang, W., Cao, Z., Xiong, D., Li, G., and Li, X. (2020). Decoding the plant genome: From epigenome to 3D organization. J. Genet. Genom. *47*, 425–435. https://doi.org/10.1016/j.jgg.2020.06.007.
10. Ouyang, W., Xiong, D., Li, G., and Li, X. (2020). Unraveling the 3D Genome Architecture in Plants: Present and Future. Mol. Plant. *13*, 1676–1693. https://doi.org/10.1016/j.molp.2020.10.002.
11. Charron, J.B.F., He, H., Elling, A.A., and Deng, X.W. (2009). Dynamic landscapes of four histone modifications during deetiolation in arabidopsis. Plant Cell *21*, 3732–3748. https://doi.org/10.1105/tpc.109.066845.
12. Willige, B.C., Zander, M., Yoo, C.Y., Phan, A., Garza, R.M., Wanamaker, S.A., He, Y., Nery, J.R., Chen, H., Chen, M., et al. (2021). PHYTOCHROME-INTERACTING FACTORs trigger environmentally responsive chromatin dynamics in plants. Nat. Genet. *53*, 955–961. https://doi.org/10.1038/s41588-021-00882-3.
13. González-Grandío, E., Álamos, S., Zhang, Y., Dalton-Roesler, J., Niyogi, K.K., García, H.G., and Quail, P.H. (2022). Chromatin Changes in Phytochrome Interacting Factor-Regulated Genes Parallel Their Rapid Transcriptional Response to Light. Front. Plant Sci. *13*, 803441. https://doi.org/10.3389/fpls.2022.803441.
14. Gu, D., Chen, C.Y., Zhao, M., Zhao, L., Duan, X., Duan, J., Wu, K., and Liu, X. (2017). Identification of HDA15-PIF1 as a key repression module directing the transcriptional network of seed germination in the dark. Nucleic Acids Res. *45*, 7137–7150. https://doi.org/10.1093/nar/gkx283.
15. Liu, X., Chen, C.Y., Wang, K.C., Luo, M., Tai, R., Yuan, L., Zhao, M., Yang, S., Tian, G., Cui, Y., et al. (2013). PHYTOCHROME INTERACTING FACTOR3 associates with the histone deacetylase HDA15 in repression of chlorophyll biosynthesis and photosynthesis in etiolated Arabidopsis seedlings. Plant Cell *25*, 1258–1273. https://doi.org/10.1105/tpc.113.109710.
16. Kim, S., Hwang, G., Kim, S., Thi, T.N., Kim, H., Jeong, J., Kim, J., Kim, J., Choi, G., and Oh, E. (2020). The epidermis coordinates thermoresponsive growth through the phyB-PIF4-auxin pathway. Nat. Commun. *11*, 1053. https://doi.org/10.1038/s41467-020-14905-w.
17. Kim, C., Kwon, Y., Jeong, J., Kang, M., Lee, G.S., Moon, J.H., Lee, H.-J., Park, Y.-I., and Choi, G. (2023). Phytochrome B photobodies are comprised of phytochrome B and its primary and secondary interacting proteins. Nat. Commun. *14*, 1708. https://doi.org/10.1038/s41467-023-37421-z.
18. Peng, M., Li, Z., Zhou, N., Ma, M., Jiang, Y., Dong, A., Shen, W.H., and Li, L. (2018). Linking phytochrome-interacting factor to histone modification in plant shade avoidance. Plant Physiol. *176*, 1341–1351. https://doi.org/10.1104/pp.17.01189.
19. Jang, I.-C., Chung, P.J., Hemmes, H., Jung, C., and Chua, N.-H. (2011). Rapid and Reversible Light-Mediated Chromatin Modifications of Arabidopsis Phytochrome A Locus. Plant Cell *23*, 459–470. https://doi.org/10.1105/tpc.110.080481.
20. Jing, Y., Guo, Q., and Lin, R. (2021). The SNL-HDA19 histone deacetylase complex antagonizes HY5 activity to repress photomorphogenesis in Arabidopsis. New Phytol. *229*, 3221–3236. https://doi.org/10.1111/nph.17114.
21. Guo, Q., Jing, Y., Gao, Y., Liu, Y., Fang, X., and Lin, R. (2023). The PIF1/PIF3-MED25-HDA19 transcriptional repression complex regulates phytochrome signaling in Arabidopsis. New Phytol. *240*, 1097–1115. https://doi.org/10.1111/nph.19205.
22. Perrella, G., Lopez-Vernaza, M.A., Carr, C., Sani, E., Gosselé, V., Verduyn, C., Kellermeier, F., Hannah, M.A., and Amtmann, A. (2013). Histone deacetylase Complex1 expression level titrates plant growth and abscisic acid sensitivity in Arabidopsis. Plant Cell *25*, 3491–3505. https://doi.org/10.1105/tpc.113.114835.

23. Mehdi, S., Derkacheva, M., Ramström, M., Kralemann, L., Bergquist, J., and Hennig, L. (2016). The WD40 Domain Protein MSI1 Functions in a Histone Deacetylase Complex to Fine-Tune Abscisic Acid Signaling. Plant Cell *28*, 42–54. https://doi.org/10.1105/tpc.15.00763.

24. Perrella, G., Carr, C., Asensi-Fabado, M.A., Donald, N.A., Páldi, K., Hannah, M.A., and Amtmann, A. (2016). The histone deacetylase complex 1 protein of Arabidopsis has the capacity to interact with multiple proteins including histone 3-binding proteins and histone 1 variants. Plant Physiol. *171*, 62–70. https://doi.org/10.1104/pp.15.01760.

25. Perrella, G., Fasano, C., Donald, N.A., Daddiego, L., Fang, W., Martignago, D., Carr, C., Conti, L., Herzyk, P., and Amtmann, A. (2024). Histone Deacetylase Complex 1 and histone 1 epigenetically moderate stress responsiveness of Arabidopsis thaliana seedlings. New Phytol. *241*, 166–179. https://doi.org/10.1111/nph.19165.

26. Zhou, N., Li, C., Xie, W., Liang, N., Wang, J., Wang, B., Wu, J., Shen, W.H., Liu, B., and Dong, A. (2024). Histone methylation readers MRG1/2 interact with PIF4 to promote thermomorphogenesis in Arabidopsis. Cell Rep. *43*, 113726. https://doi.org/10.1016/j.celrep.2024.113726.

27. Jeong, J., and Choi, G. (2013). Phytochrome-interacting factors have both shared and distinct biological roles. Mol. Cells *35*, 371–380. https://doi.org/10.1007/s10059-013-0135-5.

28. Leivar, P., and Monte, E. (2014). PIFs: Systems Integrators in Plant Development. Plant Cell *26*, 56–78. https://doi.org/10.1105/tpc.113.120857.

29. Shin, J., Kim, K., Kang, H., Zulfugarov, I.S., Bae, G., Lee, C.H., Lee, D., and Choi, G. (2009). Phytochromes promote seedling light responses by inhibiting four negatively-acting phytochrome-interacting factors. Proc. Natl. Acad. Sci. USA *106*, 7660–7665. https://doi.org/10.1073/pnas.0812219106.

30. Huq, E., and Quail, P.H. (2002). PIF4, a phytochrome interacting bHLH factor, functions as a negative regulator of phytochrome B signaling in *Arabidopsis*. EMBO J. *21*, 2441–2450. https://doi.org/10.1093/emboj/21.10.2441.

31. Rovira, A., Veciana, N., Basté-Miquel, A., Quevedo, M., Locascio, A., Yenush, L., Toledo-Ortiz, G., Leivar, P., and Monte, E. (2024). PIF transcriptional regulators are required for rhythmic stomatal movements. Nat. Commun. *15*, 4540. https://doi.org/10.1038/s41467-024-48669-4.

32. Peng, M., Li, Z., Zhou, N., Ma, M., Jiang, Y., Dong, A., Shen, W.-H., and Li, L. (2018). Linking PHYTOCHROME-INTERACTING FACTOR to Histone Modification in Plant Shade Avoidance. Plant Physiol. *176*, 1341–1351. https://doi.org/10.1104/pp.17.01189.

33. Casal, J.J., and Qüesta, J.I. (2018). Light and temperature cues: multitasking receptors and transcriptional integrators. New Phytol. *217*, 1029–1034. https://doi.org/10.1111/nph.14890.

34. Cheng, Q., Zeng, Y., Huang, S., Yang, C., Xie, Y., Shen, W.-H., and Li, L. (2024). PHYTOCHROME-INTERACTING FACTOR 7 and RELATIVE OF EARLY FLOWERING 6 act in shade avoidance memory in Arabidopsis. Nat. Commun. *15*, 8032. https://doi.org/10.1038/s41467-024-51834-4.

35. Burko, Y., Willige, B.C., Seluzicki, A., Novák, O., Ljung, K., and Chory, J. (2022). PIF7 is a master regulator of thermomorphogenesis in shade. Nat. Commun. *13*, 4942. https://doi.org/10.1038/s41467-022-32585-6.

36. Johansson, H., Jones, H.J., Foreman, J., Hemsted, J.R., Stewart, K., Grima, R., and Halliday, K.J. (2014). Arabidopsis cell expansion is controlled by a photothermal switch. Nat. Commun. *5*, 4848. https://doi.org/10.1038/ncomms5848.

37. Grefen, C., and Blatt, M.R. (2012). A 2in1 cloning system enables ratiometric bimolecular fluorescence complementation (rBiFC). Biotechniques *53*, 311–314. https://doi.org/10.2144/000113941.

38. Fang, W., Vellutini, E., Perrella, G., and Kaiserli, E. (2022). TANDEM ZINC-FINGER/PLUS3 regulates phytochrome B abundance and signaling to fine-tune hypocotyl growth. Plant Cell *34*, 4213–4231. https://doi.org/10.1093/plcell/koac236.

39. Duek, P.D., Elmer, M.V., van Oosten, V.R., and Fankhauser, C. (2004). The Degradation of HFR1, a Putative bHLH Class Transcription Factor Involved in Light Signaling, Is Regulated by Phosphorylation and Requires COP1. Curr. Biol. *14*, 2296–2301. https://doi.org/10.1016/j.cub.2004.12.026.

40. Tian, Y.-Y., Li, W., Wang, M.-J., Li, J.-Y., Davis, S.J., and Liu, J.-X. (2022). REVEILLE 7 inhibits the expression of the circadian clock gene EARLY FLOWERING 4 to fine-tune hypocotyl growth in response to warm temperatures. J. Integr. Plant Biol. *64*, 1310–1324. https://doi.org/10.1111/jipb.13284.

41. Kuno, N., Møller, S.G., Shinomura, T., Xu, X., Chua, N.-H., and Furuya, M. (2003). The Novel MYB Protein EARLY-PHYTOCHROME-RESPONSIVE1 Is a Component of a Slave Circadian Oscillator in Arabidopsis. Plant Cell *15*, 2476–2488. https://doi.org/10.1105/tpc.014217.

42. Yang, S.W., Jang, I.-C., Henriques, R., and Chua, N.-H. (2009). FAR-RED ELONGATED HYPOCOTYL1 and FHY1-LIKE Associate with the Arabidopsis Transcription Factors LAF1 and HFR1 to Transmit Phytochrome A Signals for Inhibition of Hypocotyl Elongation. Plant Cell *21*, 1341–1359. https://doi.org/10.1105/tpc.109.067215.

43. Desnos, T., Puente, P., Whitelam, G.C., and Harberd, N.P. (2001). FHY1: A phytochrome A-specific signal transducer. Genes Dev. *15*, 2980–2990. https://doi.org/10.1101/gad.205401.

44. Menon, C., Klose, C., and Hiltbrunner, A. (2020). Arabidopsis FHY1 and FHY1-LIKE Are Not Required for Phytochrome A Signal Transduction in the Nucleus. Plant Commun. *1*, 100007. https://doi.org/10.1016/j.xplc.2019.100007.

45. Millar, A.J., and Kay, S.A. (1991). Circadian Control of cab Gene Transcription and mRNA Accumulation in Arabidopsis. Plant Cell *3*, 541–550. https://doi.org/10.1105/tpc.3.5.541.

46. Tognacca, R.S., Carabelli, M., Morelli, G., Ruberti, I., and Botto, J.F. (2021). ATHB2 is a negative regulator of germination in Arabidopsis thaliana seeds. Sci. Rep. *11*, 9688. https://doi.org/10.1038/s41598-021-88874-5.

47. Zhao, L., Peng, T., Chen, C.Y., Ji, R., Gu, D., Li, T., Zhang, D., Tu, Y.T., Wu, K., and Liu, X. (2019). HY5 interacts with the histone deacetylase HDA15 to repress hypocotyl cell elongation in photomorphogenesis. Plant Physiol. *180*, 1450–1466. https://doi.org/10.1104/pp.19.00055.

48. Krahmer, J., and Fankhauser, C. (2024). Environmental Control of Hypocotyl Elongation. Annu. Rev. Plant Biol. *75*, 489–519. https://doi.org/10.1146/annurev-arplant-062923-023852.

49. Oh, E., Zhu, J.-Y., and Wang, Z.-Y. (2012). Interaction between BZR1 and PIF4 integrates brassinosteroid and environmental responses. Nat. Cell Biol. *14*, 802–809. https://doi.org/10.1038/ncb2545.

50. Patitaki, E., Schivre, G., Zioutopoulou, A., Perrella, G., Bourbousse, C., Barneche, F., and Kaiserli, E. (2022). Light, chromatin, action: nuclear events regulating light signaling in Arabidopsis. New Phytol. *236*, 333–349. https://doi.org/10.1111/nph.18424.

51. Jiao, Y., Lau, O.S., and Deng, X.W. (2007). Light-regulated transcriptional networks in higher plants. Nat. Rev. Genet. *8*, 217–230. https://doi.org/10.1038/nrg2049.

52. Perrella, G., and Kaiserli, E. (2016). Light behind the curtain: photoregulation of nuclear architecture and chromatin dynamics in plants. New Phytol. *212*, 908–919. https://doi.org/10.1111/nph.14269.

53. Bourbousse, C., Mestiri, I., Zabulon, G., Bourge, M., Formiggini, F., Koini, M.A., Brown, S.C., Fransz, P., Bowler, C., and Barneche, F. (2015). Light signaling controls nuclear architecture reorganization during seedling establishment. Proc. Natl. Acad. Sci. USA *112*, E2836–E2844. https://doi.org/10.1073/pnas.1503512112.

54. Berger, S.L. (2007). The complex language of chromatin regulation during transcription. Nature *447*, 407–412. https://doi.org/10.1038/nature05915.

55. Pikaard, C.S., and Scheid, O.M. (2014). Epigenetic regulation in plants. Cold Spring Harb Perspect Biol *6*, a019315. https://doi.org/10.1101/cshperspect.a019315.

56. Ning, Y.Q., Chen, Q., Lin, R.N., Li, Y.Q., Li, L., Chen, S., and He, X.J. (2019). The HDA19 histone deacetylase complex is involved in the regulation of

flowering time in a photoperiod-dependent manner. Plant J. *98*, 448–464. https://doi.org/10.1111/tpj.14229.

57. Benhamed, M., Bertrand, C., Servet, C., and Zhou, D.X. (2006). Arabidopsis GCN5, HD1, and TAF1/HAF2 interact to regulate histone acetylation required for light-responsive gene expression. Plant Cell *18*, 2893–2903. https://doi.org/10.1105/tpc.106.043489.
58. Bertrand, C., Benhamed, M., Li, Y.F., Ayadi, M., Lemonnier, G., Renou, J. P., Delarue, M., and Zhou, D.X. (2005). Arabidopsis HAF2 gene encoding TATA-binding protein (TBP)-associated factor TAF1, is required to integrate light signals to regulate gene expression and growth. J. Biol. Chem. *280*, 1465–1473. https://doi.org/10.1074/jbc.M409000200.
59. Carrozza, M.J., Florens, L., Swanson, S.K., Shia, W.J., Anderson, S., Yates, J., Washburn, M.P., and Workman, J.L. (2005). Stable incorporation of sequence specific repressors Ash1 and Ume6 into the Rpd3L complex. Biochim. Biophys. Acta *1731*, 77. https://doi.org/10.1016/j.bbaexp.2005.09.005.
60. Kunihiro, A., Yamashino, T., Nakamichi, N., Niwa, Y., Nakanishi, H., and Mizuno, T. (2011). PHYTOCHROME-INTERACTING FACTOR 4 and 5 (PIF4 and PIF5) Activate the Homeobox ATHB2 and Auxin-Inducible IAA29 Genes in the Coincidence Mechanism Underlying Photoperiodic Control of Plant Growth of Arabidopsis thaliana. Plant Cell Physiol. *52*, 1315–1329. https://doi.org/10.1093/pcp/pcr076.
61. Duek, P.D., and Fankhauser, C. (2003). HFR1, a putative bHLH transcription factor, mediates both phytochrome A and cryptochrome signalling. Plant J. *34*, 827–836. https://doi.org/10.1046/j.1365-313X.2003.01770.x.
62. Van Der Woude, L.C., Perrella, G., Snoek, B.L., Van Hoogdalem, M., Novák, O., Van Verk, M.C., Van Kooten, H.N., Zorn, L.E., Tonckens, R., Dongus, J.A., et al. (2019). HISTONE DEACETYLASE 9 stimulates auxin-dependent thermomorphogenesis in Arabidopsis thaliana by mediating H2A.Z depletion. Proc. Natl. Acad. Sci. USA *116*, 25343–25354. https://doi.org/10.1073/pnas.1911694116.
63. Andrews, S. (2010). FastQC: a quality control tool for high throughput sequence data (Cambridge).
64. Bolger, A.M., Lohse, M., and Usadel, B. (2014). Trimmomatic: a flexible trimmer for Illumina sequence data. Bioinformatics *30*, 2114–2120. https://doi.org/10.1093/bioinformatics/btu170.
65. Langmead, B., and Salzberg, S.L. (2012). Fast gapped-read alignment with Bowtie 2. Nat. Methods *9*, 357–359. https://doi.org/10.1038/nmeth.1923.
66. Ramírez, F., Ryan, D.P., Grüning, B., Bhardwaj, V., Kilpert, F., Richter, A. S., Heyne, S., Dündar, F., and Manke, T. (2016). deepTools2: a next generation web server for deep-sequencing data analysis. Nucleic Acids Res. *44*, W160–W165. https://doi.org/10.1093/nar/gkw257.
67. Zhang, Y., Liu, T., Meyer, C.A., Eeckhoute, J., Johnson, D.S., Bernstein, B. E., Nusbaum, C., Myers, R.M., Brown, M., Li, W., and Liu, X.S. (2008). Model-based Analysis of ChIP-Seq (MACS). Genome Biol. *9*, R137. https://doi.org/10.1186/gb-2008-9-9-r137.
68. Heinz, S., Benner, C., Spann, N., Bertolino, E., Lin, Y.C., Laslo, P., Cheng, J.X., Murre, C., Singh, H., and Glass, C.K. (2010). Simple Combinations of Lineage-Determining Transcription Factors Prime cis-Regulatory Elements Required for Macrophage and B Cell Identities. Mol. Cell *38*, 576–589. https://doi.org/10.1016/j.molcel.2010.05.004.
69. Carroll, T.S., Liang, Z., Salama, R., Stark, R., and de Santiago, I. (2014). Impact of artifact removal on ChIP quality metrics in ChIP-seq and ChIP-exo data. Front. Genet. *5*, 75.
70. Wang, Q., Li, M., Wu, T., Zhan, L., Li, L., Chen, M., Xie, W., Xie, Z., Hu, E., Xu, S., and Yu, G. (2022). Exploring Epigenomic Datasets by ChIPseeker. Curr. Protoc. *2*, e585. https://doi.org/10.1002/cpz1.585.
71. Yu, G., Wang, L.-G., Han, Y., and He, Q.-Y. (2012). clusterProfiler: an R Package for Comparing Biological Themes Among Gene Clusters. OMICS *16*, 284–287. https://doi.org/10.1089/omi.2011.0118.
72. Stark, R., and Brown, G. (2011). DiffBind differential binding analysis of ChIP-Seq peak data. In R package version 100.
73. Schindelin, J., Arganda-Carreras, I., Frise, E., Kaynig, V., Longair, M., Pietzsch, T., Preibisch, S., Rueden, C., Saalfeld, S., Schmid, B., et al. (2012). Fiji: an open-source platform for biological-image analysis. Nat. Methods *9*, 676–682. https://doi.org/10.1038/nmeth.2019.
74. Geelen, D., Leyman, B., Batoko, H., Di Sansebastiano, G.-P., Moore, I., and Blatt, M.R. (2002). The Abscisic Acid–Related SNARE Homolog NtSyr1 Contributes to Secretion and Growth: Evidence from Competition with Its Cytosolic Domain. Plant Cell *14*, 387–406. https://doi.org/10.1105/tpc.010328.
75. Perrella, G., Davidson, M.L.H., Donnell, L.O., Nastase, A.-M., Herzyk, P., Breton, G., Pruneda-Paz, J.L., Kay, S.A., Chory, J., and Kaiserli, E. (2018). ZINC-FINGER interactions mediate transcriptional regulation of hypocotyl growth in Arabidopsis. Proc. Natl. Acad. Sci. USA *115*, E4503–E4511. https://doi.org/10.1073/pnas.1718099115.
76. Martignago, D., da Silveira Falavigna, V., Lombardi, A., Gao, H., Korwin Krukowski, P., Galbiati, M., Tonelli, C., Coupland, G., and Conti, L. (2023). The bZIP transcription factor AREB3 mediates FT signalling and floral transition at the Arabidopsis shoot apical meristem. PLoS Genet. *19*, e1010766. https://doi.org/10.1371/journal.pgen.1010766.

STAR★METHODS

KEY RESOURCES TABLE

REAGENT or RESOURCE	SOURCE	IDENTIFIER
Antibodies		
Goat polyclonal anti-PIF4	Agrisera	Cat# AS163955
Rabbit polyclonal anti-PhyB	Agrisera	Cat# AS214566
Rabbit polyclonal anti-UGPase	Agrisera	Cat# AS05086; RRID:AB_1031827
Rabbit polyclonal anti-GFP	Abcam	Cat# Ab290; RRID:AB_303395
Rabbit polyclonal anti-HA	Abcam	Cat# Ab9110; RRID:AB_307019
Rabbit polyclonal anti-RFP	Abcam	Cat# Ab62341; RRID:AB_945213
Rabbit polyclonal anti-H3K27Ac	Abcam	Cat# Ab4729; RRID:AB_2118291
Rabbit polyclonal anti-H3K9K14Ac	Diagenode	Cat# pAb-005-050
Bacterial and virus strains		
DH5α Chemically Competent Cells	ThermoFisher	Cat# 18265017
GV3101 Electrocompetent Cells	Fisher scientific	Cat# NC2385797
Chemicals, peptides, and recombinant proteins		
Protein-A-Dynabeads	ThermoFisher	Cat# 10002D
Proteinase K	ThermoFisher	Cat# EO0491
cOmplete Proteinase inhibitor cocktail tablet	Roche	Cat# 11836170001
MG132	ThermoFisher	Cat# J63250.MCR
Critical commercial assays		
μMACS™ Anti-GFP Starting Kit	Miltenyi Biotec	Cat# 130-091-288
Deposited data		
ChIP seq of H3K9K14Ac and H3K27Ac in WT and *hdc1-1*	This study	BioProject: PRJNA1191197
Experimental models: Organisms/strains		
Arabidopsis: Col-0	Perrella et al.[22]	NA
Arabidopsis: *hdc1-1*	Perrella et al.[22]	NA
Arabidopsis: *35S:HDC1*	Perrella et al.[22]	NA
Arabidopsis: Ubi10:GFP-HDC1	Perrella et al.[22]	NA
Arabidopsis: *pif4-2*	Fang et al.[38]	NA
Arabidopsis: *pif4 pif5*	Fang et al.[38]	NA
Arabidopsis: *phyB-9*	Fang et al.[38]	NA
Arabidopsis: *35S:PIF4-HA*	Van Der Woude et al.[62]	NA
Oligonucleotides		
Primers are listed in Table S1		
Recombinant DNA		
nYFP-HDC1	This study	
cYFP-H1	Perrella et al.[24]	
cYFP-PIF4	This study	
cYFP-PIF5	This study	
nYFP-RXT3L	This study	
GFP-HDC1	Perrella et al.[22]	
RFP-PIF4	This study	
Software and algorithms		
FastQC	Andrews[63]	
Trimmomatic v0.39	Bolger et al.[64]	
Bowtie2 v2.5.0	Langmead et al.[65]	

(*Continued on next page*)

Continued

REAGENT or RESOURCE	SOURCE	IDENTIFIER
deepTools2	Ramírez et al.[66]	
Macs2 v2.2.7	Zhang et al.[67]	
Homer	Heinz et al.[68]	
ChIPQC	Carrol et al.[69]	
ChIPseeker v1.34.1	Wang et al.[70]	
ClusterProfiler v3.0.4	Yu et al.[71]	
DiffBind v3.8.4	Stark et al.[72]	
GraphPad	Prism	
ImageJ	Schindelin et al.[73]	

EXPERIMENTAL MODEL AND STUDY PARTICIPANT DETAILS

All *Arabidopsis thaliana* plants used in this study are of the Columbia (Col-0) ecotype unless stated otherwise. Double mutant combinations of *hdc1-1*, *35S:HDC1* (referred to as OXHDC1), *35S:PIF4:HA* with mutants of other genes (*pif4-2*, *pif4pif5*, *phyB-9*) and Ubi10:GFP-HDC1 lines were generated by crossing or *Agrobacterium tumefaciens* strain GV3101-mediated transformation, respectively. *PhyB-9*, *pif4-2 pif5-3*, *pif4-2* and 35S:PIF4-HA were kindly provided by Eirini Kaiserli and Martijn Van Zanten, respectively. Primer sequences to genotype the mutants were previously described.[38,62]

METHOD DETAILS

Plant materials and growth conditions

For each experiment Arabidopsis seeds were surface sterilized and stratified. Surface sterilizing was conducted by vortex in 50% sodium hypochlorite solution, followed by three washes with double distilled sterile water (ddH_2O). Stratification was conducted at 4°C for 2–3 days in darkness. All the seeds were sown on half-strength Murashige and Skoog (MS) medium (pH 5.7) with 0.8% plant agar.

Hypocotyl measurements

Surface-sterilized and stratified seeds were first exposed to white light (60 μmol m^{-2} s^{-1}) for 4 h to synchronize and induce germination prior to exposure to the various specific light conditions described in the figure legends before hypocotyl measurements were recorded. Seedlings were scanned on the end of the fifth day post-germination as described in Fang et al., 2022.[38] Hypocotyl length was measured from digital images using the ImageJ software (Fiji, NIH).[73] An average of 15 seedlings was measured for each treatment for at least three experimental replicates. Data were plotted and statistical analyses were performed using GraphPad Prism. In whisker plots, boxes show median, interquartile range (IQR) and maximum-minimum interval of each dataset together with individual data points. Data shown are representative of three biological replicates with independent populations of seedlings exposed to an identical treatment.

qRT-PCR analysis

Total RNA was extracted from approximately 100 mg of 4-day-old seedlings (or as indicated in the figure legend) with the RNeasy plant mini kit (Qiagen). Tissue was frozen in liquid nitrogen and was ground using a tissue Lyser (Qiagen). First-strand cDNA was obtained from 1 μg total RNA using a QuantiTect reverse transcription kit (Qiagen) following the manufacturer's instructions. Quantitative PCR (qRT-PCR) was performed with TB Green Premix Ex Taq (Takara) on a CFX96 Real-Time PCR machine (Biorad). Primers used are reported in Table S1. The cycling program was performed as follows: 3min at 95°C, followed by 45 cycles of 10s at 95°C, 30 s at 59.5°C, the cycling was finished by 3 s at 65°C and 30 s at 95°C, 12°C in hold. Data analysis was conducted as reported in Perrella et al., 2024.[25] The expression of each gene of interest was normalized to the housekeeping gene *IRON SULFUR CLUSTER ASSEMBLY 1* (*ISU*) or subsequently to other controls as indicated in figure legends.

Western blotting

Approximately 100 mg of 5-day-old Arabidopsis light-grown pooled seedling tissue (or as indicated in the figure legend) was used for total protein isolation. Finely ground tissue powder was dissolved in 1.5 volumes of 4×Laemmli buffer (250 mM Tris-HCl pH 6.8, 10% [w/v] SDS, 20% [v/v] β-mercaptoethanol, 40% [v/v] glycerol, 0.1% [w/v] bromophenol blue). After vortex, the mixture was boiled at 100°C for 5 min prior to centrifugation for 1 min at 13,000 rpm. The supernatant was used for SDS-PAGE analysis. Equal volumes of total protein were separated in SDS-PAGE (Invitrogen Bolt 4–12% Bis-Tris Plus) or 10% gels made from acrylamide, followed by transfer and immunodetection using specific antibodies (details are given in figure legends) as previously described.[38] Primary

antibodies used in this study were anti-PIF4 (1:1,000 [v/v], Agrisera AS163955), anti-phyB (1:1,000 [v/v], Agrisera AS214566), anti-GFP (1:3,000 [v/v] Abcam ab290), anti-HA 1:1,000 [v/v] Abcam ab9110), anti-UGPase (1:10,000 [v/v], Agrisera AS05086), anti-RFP (Abcam ab62341). Protein levels were quantified by band intensities with ImageJ.

BiFC

The Gateway Cloning System (Invitrogen Life Technologies) was used to create vectors for BiFC. Vector constructions of nYFP-HDC1, nYFP-RXT3L, cYFP-PIF4, cYFP-PIF5 were generated using primers designed specifically for each gene of interest. Constructions generated in 2in1 vectors[37] were transformed to Agrobacterium GV301 strain and were used for BiFC. All constructs were verified by sequencing using the appropriate primers (see Table S1).[24] Cell culture of each combination was then infiltrated in *Nicotiana benthamiana* leaves as previously described.[74] The infiltrated plants were transferred to a growth room cabinet under white light for a period of 2–3 days post-incubation before examination by confocal microscopy.

Co-IP

Co-immunoprecipitation in Arabidopsis was conducted by using μMACS GFP Isolation kit (Miltenyi Biotec).[75] Whole tissue was frozen and ground in liquid nitrogen. Finely ground powder was dissolved in 1.5 volumes of lysis buffer [93.2mM Na2HPO4, 68mM NaH2PO4, 150mM NaCl, 5mM EDTA, 0.1% Triton-100, supplemented with freshly added 50 μM MG132, 1mM PMSF and 1× protease inhibitor cocktail tablet (Roche) just before use] and mixed by rotating at 4°C for 15 min. Finely mixed tissue was centrifuged at 4°C for 10min at 10000 rpm. For each genotype, supernatant containing 1.2 mg protein was incubated with 50 μL μMACS Anti-GFP MicroBeads for 45 min. Bradford assay was conducted to evaluate the concentration of protein. Sample was then loaded onto a MACS Column placed in the magnetic field and beads were washed through the column by following the manufacturer's instructions. GFP-tagged protein was finally eluted by pre-warmed (95°C) elution buffer. The precipitated proteins were analyzed by SDS-PAGE and western blot. Native protein was loaded together as control.

Co-immunoprecipitation in *Nicotiana benthamiana* after leaf infiltration was conducted as previously described.[76] In detail, total proteins were extracted in lysis buffer (50 mM Tris pH 7.5, 150 mM NaCl, 10% Glycerol and 2 mM EDTA supplemented with 5 mm DTT, 0.2% Triton and proteinase inhibitors. The extract was incubated overnight at 4°C with GFP-sepharose beads (Cromotek). After several washes, the beads were boiled in Laemmli Buffer for 5 min before loading the acrylamide gel.

Chromatin immunoprecipitation (ChIP) and ChIP PCR

Chromatin immunoprecipitation was performed with 2 g of tissue as previously described.[25] Approximately 2g of fresh tissue was collected and fixed with 1% formaldehyde under vacuum for 15min. Bioruptor sonicator (B01020001; Diagenode, Seraing (Ougrée), Belgium) was used to shear the chromatin using the following settings: 40 cycles of 30 s ON, 20 s OFF at high power. Anti-H3K9K14Ac and H3K27Ac antibodies were used to IP the chromatin (Diagenode pAb-005-050 and Abcam ab4729). IP DNA was quantified by Qubit (Thermofisher). For each antibody the experiment was conducted by two experimental replicates.

ChIP-qPCR was performed at the following cycles: 95°C 3 min, 95°C 3 s, 59.5°C 30 s (40 cycles), 95°C 91 min, and 60°C 30 s (Melting curve). Reactions were performed on four technical replicates and three independent biological replicates. Relative enrichment for ChIP-qPCR assays was calculated, as shown in Perrella et al., 2024.[25] Histone H3K9K14 and H3K27 acetylation enrichment over loci were determined by normalising immunoprecipitated DNA against input DNA (genomic) for the regions highlighted in Figure 5 and indicated as percentage of nuclear DNA (% Input). Primer sequences are reported in Table S1. Primer positions are indicated in Figure 5.

ChIP sequencing and data processing

Sequencing of the ChIP DNA was carried out by Mentotech s.r.l. ChIP Illumina Library preparation was performed using a Novaseq 6000, paired-ends 150 million of reads and 8 Gbp per sample.

To assess the quality of the raw ChIP-seq data, we used the FastQC tool v0.11.4.[63] This was followed by trimming adapter sequences and filtering out low-quality bases, setting a minimum quality score of 25, and discarding reads shorter than 35 bases with Trimmomatic v0.39.[64] Then, we performed a quality reassessment of the trimming step with FastQC. High quality reads that were obtained after the trimming step were mapped against the TAIR10 genome (Plant Ensembl release 58) using the bowtie2 v2.5.0 aligner.[65] Reads were then marked for duplicates using the Picard command line tool MarkDuplicates v3.1.1 and filtered using a mapping quality minimum threshold of 30. BigWig files were generated for genome wide visualization of the peaks using deeptools' bamCoverage v3.5.2[66] with the following options: "–normalizeUsing BPM –binSize 50". The software macs2 v2.2.7.1[67] was used for the peak calling in narrow mode and without inputs with the following options: "-g 1.2e8 -q 0.05". Consensus peaks were later generated by using the HOMER software and its submodule mergePeaks to keep peaks coming from the two replicates (Data S1).[68]

To assess the quality of the ChIP-seq experiment, several metrics were computed using the ChIPQC[69] package. The metrics were computed on chromosome 1 to reduce the computational time cost. BAM files from replicates were merged into single files and a BigWig file was generated for each condition with the same options as before. A combination of Deeptools compute Matrix (–before Region Start Length 3000 –region Body Length 5000–after Region Start Length 3000 –skipZeros) and plot Profile were used to plot the peak profile around the Transcription Starting Site (TSS) and Transcription Ending Site (TES).

The ChIPseeker package v1.34.1[70] was used to annotate the peaks using the Araport11 annotation; the promoter region was selected as ±3kb from the TSS. A Gene Ontology (GO) analysis was performed for each peak category (Common, Unique in Mutant and Unique in Wild Type) for each histone mark (H3K27Ac and H3K9K14Ac) with the clusterProfiler package v3.0.4.[71] We applied a *p*-value cutoff of 0.05 and an adjusted *p*-value cutoff of 0.05. From the defined peakset and for each histone mark, we focused on the peaks shared between the Mutant (Mut) and Wild Type (WT). We conducted a differential enrichment analysis on the common peaks using DiffBind v3.8.4.[72] The Differently expressed peaks were found using a minimum FDR threshold value of 0.05. Finally, we performed another GO analysis on the up- and down-significantly enriched genes (Data S2 and S3).

Confocal imaging and analysis

Seedlings or leaf disks onto slides containing a droplet of dH2O (without fixation) were imaged under a A1R confocal microscope (Nikon).

The leaf epidermal cells were obtained using 20× or 63× immersion objectives depending on the specific experiment. GFP, YFP and RFP signals were assessed in *N. benthamiana* epidermal cells two days after infiltration.[22] EGFP fluorescence was excited at 488 nm using a GaAsp laser scan long-pass filter and collected at 508–541 nm. EYFP fluorescence was excited at 488 nm and collected at 516–551 nm. Texas Red signal was excited at 561 nm and collected at 598–634 nm.

For Arabidopsis seedlings, eCFP signal was excited at 445nm and collected at 463-516nm.

QUANTIFICATION AND STATISTICAL ANALYSIS

All experiments were conducted with at least three biological replicates or otherwise stated in the figure legends. Number of samples, mean and standard deviation is reported on the figure legends.

Statistical analysis and plotting were conducted using ANOVA one way or T test by using Excel, SPSS Statistics, and GraphPad Prism software. *p*-values $\leq$0.05 were considered statistically significant.